

Evolutionary bursts drive morphological novelty in a continental radiation of skinks



5

Morphological novelty evolves by bursts in a continental radiation of skinks

10

Ian G. Brennan ^{*1}, David G. Chapple²,
J. Scott Keogh¹, Stephen Donnellan^{3,4}

¹Division of Ecology & Evolution, Research School of Biology,
Australian National University, Canberra, ACT 2600 Australia

²School of Biological Sciences, Monash University
Clayton, VIC Australia

³ School of Biological Sciences, The University of Adelaide,
Adelaide, SA Australia

⁴South Australian Museum, North Terrace, Adelaide SA 5000 Australia

Short Title: Morphological evolution in Egerniinae skinks

*Corresponding author: ian.brennan@anu.edu.au

Abstract

Animals come in all shapes and sizes. From mundane to bizarre, their features are the result
15 of millions of years of evolution and mutation accumulating differences and adjusting designs.
But bodies are complex structures composed many regions that serve varied functions following different evolutionary paths. As a result of differing selective pressures and functional
constraints phenotypes evolve and diverge. However there is little consensus about the evolutionary mode of most traits and if novel morphologies evolve from prolonged or episodic
20 divergences. Here we use novel exon-capture and linear morphological datasets to investigate the tempo and mode of morphological evolution in Australo-Melanesian *Egerniinae* skinks. By collecting a morphological dataset that encompasses the lizard body plan we are able to identify that most traits evolve conservatively it infrequent evolutionary bursts result in morphological novelty. These phenotypic discontinuities occur via rapid rate increases along
25 individual branches, inconsistent with both gradualistic and punctuated equilibrial evolutionary modes. Instead, this ‘punctuated gradualism’ has resulted in the rapid evolution of blue-tongued giants and armored dwarves in the ~20 million years since colonizing Australia. These results outline the evolutionary pathway towards new morphologies and highlight the heterogeneity of evolutionary tempo and mode.

30

Note: Pagel et al. (2022) make a convincing argument for a model (*fabric*) in which you can have great changes in traits evolve via biased gradual (directional) walks, without the need for increasing evolutionary rate (most of the time). While it's worth considering I am not convinced reanalyzing the entire dataset is necessary the inference of discontinuous
35 trait evolution still holds.

Elaboration vs. Innovation: Following Endler et al. (2005) and Guillerme et al. (2023). Major axis of variation (elaboration) across the whole skink body-plan is primarily tail length (not size!), with primary innovation occurring via variation in interlimb length. Regardless
40 of phylogenetic scale the major axis remains the same (tail length), however innovation occurs along different axes depending on clade (interlimb for *Tiliqua/Cyclodomorphus*, size for *Bellatorias/Egernia* and *Liopholis*). Suggests different ecological pressures influence differentiation within clades, e.g. niche partitioning by size vs habitat partitioning by tail length.

Introduction

- 45 Great variations in organismal morphology are expected to accumulate over long periods of time and reflect the varied requirements of different species [CITE Foote 1997; Deline et al. 2018]. Some organisms are very small and some are very large, others are brightly colored and others cryptic, and through drift and selection, traits respond and diverge from common forms. But despite the dramatic variation we see in nature, when we look closely,
- 50 measures of these differences (variance, disparity, *et al.*) almost always fail to exceed the expectation of a neutral model where the accumulation of variation is the result of a random evolutionary walk through time (Brownian Motion) [CITE Lynch 1990; Hansen & Houle 2004]. In other words, Earth's flora and fauna realize only a fraction of all possible shapes and sizes [CITE Hall 1996]. This diversity undershoot suggests bounds on phenotypes as a
- 55 result of genetic, functional, or developmental constraints [CITE]. If this is the case, then how do novel morphologies arise? And what does the mode of morphological evolution look like if not gradual?

When traits are assumed to evolve under an unbiased random walk (Brownian Motion), trait variance (v) is proportional to evolutionary rate (σ^2), and the accumulation of variance is dictated by elapsed time (t ; so $v=\sigma^2 t$). This exploration of trait space (diffusion) is characterized by trait change along branches drawn from a normal (Gaussian) distribution, and assumes a flat adaptive landscape [CITE Arnold et al. 2001 Genetica; Hansen & Martins 1996]. Given observed trait limits, correlations among traits, and the “clumpiness” of extant morphological diversity, this seems an unlikely expectation [CITE Felsenstein 1988; Deline et al. 2018]. In practice, morphological evolution is often concentrated on one or a small number of major axes. The primary axis serves as a ‘line of least resistance’ [CITE Schlüter 1996] providing a pool of variation on which selection can act. However evolution is not limited to the major axis, and trajectories along minor axes may also pave a path towards new phenotypes. These competing processes have been termed “elaboration” (*along* major axis) and “innovation” (*away* from major axis) [CITE Endler et al. 2005; Guillerme et al. 2023]. However their relative contributions towards organismal macroevolution and the evolution of novel forms has been largely overlooked [CITE Guillerme et al. 2023].

Almost 80 years ago G.G. Simpson suggested this occurred by rapid “jumps” to new adaptive zones across an uneven landscape [Simpson 1944]. One pathway there requires relaxing our assumption that traits evolve consistently across lineages—changing the *mode* of evolution. Proposed alternative evolutionary models such as pulsed or punctuated processes account for rapid jumps in just such a way—by deviating only in the evolutionary *mode*—leaving variance to accumulate as under BM. Another pathway however requires relaxing our assumption that traits evolve via constant rates through time—changing the *tempo* of evolution. This is often implemented in Variable Rates or Multi-Regime models of trait evolution. Traditionally, jumps have been difficult to identify without fossil data. This is due in part to the limited information content at internal nodes of a phylogenetic tree, however, even in fossil studies debate has continued about gradual versus pulsed/punctuated evolution [Hunt 2008; Hunt et al. 2015]. Recent advances in phylogenetic comparative methods however, provide the tools to distinguish between gradual and punctuated evolutionary modes, and suggest that pulsed evolution and rate heterogeneity may be a common processes [CITE Uyeda et al. 2011; Landis et al. 2013; Baker et al. 2016; Landis & Schraiber 2017; Bastide

& Didier 2023].

When studying the morphological evolution of any empirical group differences in evolutionary mode and tempo are potentially compounded by mosaic evolution—which suggests that processes may vary widely across individual traits and the modules they make up. So when looking for macroevolutionary shifts towards new phenotypes, changes may be temporally, phylogenetically, or regionally (across the body) heterogenous. **Something about how major/minor axes of variation may change across groups.** Just a century ago these complications seemed insurmountable. “To select a few of the great number of structural differences for measurement would be almost certainly misleading; to average them all would entail many thousands of measurements for each species or genus compared” [CITE Matthew 1914]. Modern comparative methods however, have made these comparisons possible. Here we investigate the relative roles these sources of variation play, by focusing on the egerniinae skinks. Egerniines consist of ~60 species with varied ecologies, high levels of sociality [CITE Chapple 2005; Gardner et al. 2008], and highly imbalanced biogeographic richness. The majority of species (~48 spp.) are endemic to Australia where their distributions span the continent’s highest alpine peaks and most inhospitable deserts. To survive in such varied climes, egerniines have diverged into herbivorous giants that roam the treetops, spiky socialites that live communally in rock crevices or complex burrows, and elongate long-lived slow-movers that wander across open lands. But to what degree are these morphological deviations *remarkable*, and what tempo and mode have they evolved by? To answer these questions we started by generating an exon-capture dataset for egerniinae skinks and reconstructing the phylogenetic relationships of this group. To look at morphological evolution we collected an extensive phenotypic dataset of 21 linear measurements which summarize broad axes of variation across the head, body, limbs, and tail. Finally we incorporate these data into a multivariate framework for comparing evolutionary rates and disparity of traits (and the modules they compose) relative to a neutral BM model of evolution. From this we are able to show that (1) most traits show heterogeneous—not neutral or incremental—evolutionary histories, (2) evolutionary bursts are temporally and phylogenetically distributed but uncommon, and (3) these jumps result in morphological novelty that can exceed uncorrelated trait expectations.

Methods

Walkthroughs of the data, code, analyses, and results are available in the *Supplementary Material*, on GitHub at www.github.com/IanGBrennan/EgerniaEvolution, and from the Dryad Digital Repository: [http://dx.doi.org/10.5061/dryad.\[NNNN\]](http://dx.doi.org/10.5061/dryad.[NNNN]) (to be updated)

Data Collection

We assembled an exon-capture dataset across 77 egerniinae skinks representing 48 of 60 currently recognized species, with a focus on Australian taxa (45 of 48 spp.). This sampling covers all 8 genera, as well as many recognized subspecies ([Table S1](#)). We included a single outgroup skink *Eutropis longicaudata*. Nuclear exons were targeted and sequenced using the Anchored Hybrid Enrichment approach (Lemmon *et al.* 2012), and resulted in 379 loci

(average coverage 367 loci, min = 362, max = 375) totaling ~600 kbp per sample (Fig.[S2](#)). Rough alignments were compiled using MAFFT [CITE MAFFT] and refined using MACSE [CITE MACSE], alignment parameters are specified in the supplementary materials. Per locus information content is summarized in Fig.[S3](#).

We collected 21 linear measurements for 61 egerniinae skink species from 650 museum samples (average 10 per spp., min.=2, max.=134). These linear measurements aimed to capture the gross morphology of the lizard body plan and are distributed across the head, body, limbs, and tail (Fig.[S4](#)). From the initial 21 measurements some were further divided (e.g. snout-vent length) or dropped to arrive at a set of 19 non-overlapping morphological traits that are summarized in the Supplemental Material ([Morphological Measurements](#)).

Phylogenetic Analyses

We reconstructed individual genealogies for our exon-capture data (n=379) under maximum-likelihood in IQTREE (Schmidt *et al.* 2014), allowing the program to assign the best fitting model of molecular evolution using PartitionFinder, then perform 1,000 ultrafast bootstraps (Haeseler *et al.* 2013). We then estimated the species tree using the shortcut coalescent method ASTRAL III (Zhang *et al.* 2017), with IQTREE gene trees as input. For comparison we estimated a locus-partitioned concatenated species tree in IQTREE. To estimate divergence times among taxa we applied a series of fossil and secondary calibrations in MCMCTree [CITE MCMCTree] as outlined in [Table S2](#). We started by concatenating all loci and partitioning them into two partitions, first and second codons together, and third codons separately, then used *baseml* to get the approximate likelihoods before running *mcmcTree* on the gradient and Hessian (in.BV file) for four replicate analyses. We compared mcmc files for stationarity and convergence, combined them using *logCombiner* [CITE logCombiner], and used this combined mcmc file to summarize divergence times on our tree (*print* = -1 in .ctl file).

Phenotypic Analyses

Our interest is in identifying the tempo and mode of evolution that produces morphological novelty and so we focus on the dynamics of morphological diversification in the egerniinae radiation. Our approach is based on a novel dataset that summarizes the lizard body plan. We started by generating mean trait values per species and removed the effect of absolute size by transforming our trait values into log-shape ratios. To identify independently evolving morphological modules we designed module models that ranged from highly specialized (head, limbs, body, and tail traits evolve independently) to highly integrated (null model in which all traits belong to a single module), see Supplementary Material for details. We compared model likelihoods and estimated correlation coefficients using *EMMLi* and used the preferred model to designate module-specific datasets.

To identify the evolutionary mode of individual morphological traits we fit a series of models ranging from a basic unbiased random walk to entirely punctuated. These allowed phenotypes to evolve through incremental change (Brownian Motion), incremental change around an optimum (Ornstein Uhlenbeck), decreasing change with time (Early Burst)—akin to an adaptive radiation scenario, two “pulse” or “jump” models which allow change

in instantaneous bursts (Jump Normal, Normal Inverse Gaussian), and a Variable Rates
170 model in which rates of change vary across individual branches of the tree—similar to the relaxed clock model of timetree estimation. We fit the BM, OU, EB, JN, and NIG models in *pulsR* (Landis & Schraiber, 2017). We fit the VR model in *BayesTraits V3* and processed the output using the standalone *PPPostProcess* software. We compared model fit by AIC scores. *BayesTraits* implements an MCMC algorithm so to estimate a maximum likelihood
175 for the VR model we transformed the input tree by the estimated median rate scalar, then fit the observed data to the transformed tree using BM in *pulsR*. We obtained an AIC value by penalizing the likelihood for each scaled branch of the transformed tree with mean scalar r greater than two, in addition to the estimation of the rate parameter and root state. We then calculated AICw for each model and identified a preferred model if its AICw was greater
180 than twice the next best model.

To understand the temporal and phylogenetic heterogeneity of evolution we estimated ancestral states for each trait under the rate heterogeneous VR model by optimizing Brownian Motion on the VR rate-transformed trees in *phytools*. We extrapolated trait values linearly along branches given start and end values at nodes and a constant evolutionary rate. We
185 did this from the root to the tips in 0.1 million year windows across all branches (using the function *trait.at.time*). To summarize the standing morphological variation across the same temporal windows we calculated disparity as both the variance and the average squared Euclidean distance among all pairs of contemporaneous taxa (using *extract.variance*). Similarly we extracted the mean evolutionary rate in 0.1 million year windows for each trait and
190 module (using *extract.stat*). To determine if our observed patterns follow a null expectation of the accumulation of disparity through time we simulated univariate and uncorrelated and correlated multivariate datasets for each trait and module applying parameter estimates from observed data for theta, sigma, and covariance. We carried out the same disparity and rate through time extraction methods in 0.1 million year windows. To understand the relative
195 contribution of niche expansion and niche packing to the accumulation of disparity through time we compared slopes of the accumulation of variance of observed traits and modules to simulated data. We plotted the trends in variance, rate, and slopes using custom functions found in the scripts included in the supplement.

Lastly, to summarize the major avenues of morphological change we ran PCA on (1)
200 all traits jointly and across (2) individual modules and (3) clades separately, then fit linear models to the first 2 PC axes (always accounting for $\geq 90\%$ of variance). This allowed us to identify the major axes of elaboration (PC1) and innovation (PC2) following the language of [CITE Endler et al. 2005] and [CITE Guillerme et al. 2023]. Tracking the angle and extent of trait change between individual nodes enabled us to qualitatively identify periods
205 of primarily innovation or elaboration on a branch-by-branch basis. **This last paragraph could probably be moved forward, but I'll leave it here for now**

Results

Phylogenetic Analyses

Concatenated (Fig.S7) and coalescent species trees (Fig.1) return broadly similar topologies with the exception of a handful of extremely short internal branches (Fig.S8). These discordant branches fall within the anomaly zone [CITE Linkem et al. 2016] in which concatenation is likely to be misled by the contribution of a large number of anomalous gene trees. In support of this, these nodes as represented in our coalescent species tree generally have low gene concordance factors (gCFs) and equivocal site concordance factors (sCFs), but are strongly supported by individual topology tests (see Supplementary Materials [Topology Tests](#)). Of these contentious nodes, two have taxonomic implications. *Lissolepis* is not recovered as monophyletic, with *L. coventryi* estimated as sister to *Liopholis*, and *L. luctuosa* more closely related to the remaining egerniines (*Cyclodomorphus*, *Tiliqua*, *Bellatorias*, *Egernia*). We also find *Cyclodomorphus* to be non-monophyletic, with the *C. gerrardii* group more closely allied with *Tiliqua* than with the *C. maximus* group.

Branches that define many of the inter-generic relationships among Australian egerniines are the result of rapid speciation events. Most of these branches are shorter than a million years long, and several of which are less than 500k years long. These rapid divergences contrast with the deep splits between Australian egerniines and their sister taxon *Corucia* (30 mya), as well as the preceding split from *Tribolonotus* (60 mya) (Fig.1,S1).

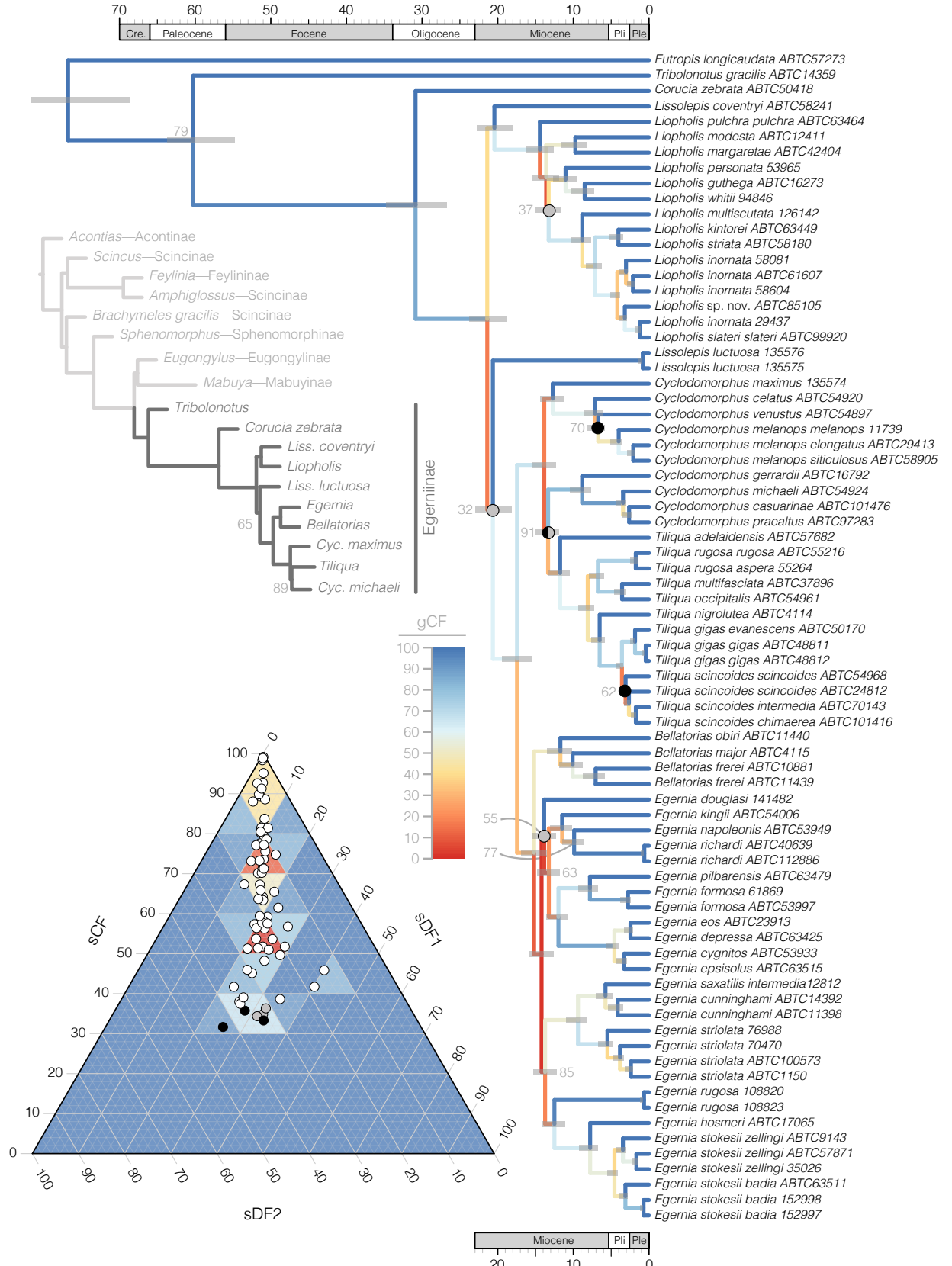


Figure 1: Species tree caption below.

Figure 1. The species tree estimated with ASTRAL and time-calibrated with MCMCTree shows late Oligocene or early Miocene divergences of most major Australian egerniinae skinks, in contrast to a Paleocene divergence from *Tribolonus* and early Oligocene divergence from the monotypic *Corucia*. Local posterior supports for all nodes are 100, except where indicated by grey numbers.

230 Branches are colored according to gene concordance factors (gCF)—the proportion of gene trees which decisively support the given bifurcation—as estimated by iqtree. The ternary plot bottom left shows the distribution of site concordance factors (sCF) for all nodes in the presented tree. sCFs provide another way of interpreting uncertainty by showing relative support for alternative resolutions of a given bifurcation (sDF1, sDF2). sCF values plotted in black on the ternary plot

235 and corresponding tree highlight nodes where $sCF < sDF1$ or $sCF < sDF2$, meaning the bifurcation presented on the tree is not supported by the majority of sites in the concatenated alignment. sCF values plotted in grey on the ternary plot and corresponding tree highlight nodes where $sCF \approx sDF1 \approx sDF2$, suggesting an unresolved polytomy.

Phenotypic Analyses

240 Modularity and integration model selection in *EMMLi* identified a four module model with separate within module correlations (intramodule integration varies among modules) and separate among module correlations (intermodule integration varies among modules) as the best fit to our data.

245 Thirteen of nineteen morphological traits are best fit by variable rate or pulsed models (Fig.S6). The abundant preference for heterogeneous evolutionary models encouraged us to focus on the evolution of traits and modules under the Variable Rates model for all further analyses. The major axis of morphological variation (elaboration; PC1) across the Egerniinae and acroos each genus is primarily explained by tail length (Fig.SXX-loadings). The major axis of morphological innovation (PC2) varies when considering the clade as a 250 whole (interlimb length) or individual genera (primarily size and/or interlimb length). We visualize this through varied slopes between our first two PC axes, highlighting different paths to phenotypic novelty (Fig.2).

With few exceptions, trait variance accumulated more slowly through the first 40 million years of egerniine evolution than under the BM null model, for both individual traits 255 (Fig.S16) and modules (Fig.3). Comparing the slopes of these accumulation curves highlights periods of significant morphological conservatism (tail module 20–15 mya) and expansion (body and limb modules 18–14 mya; tail module 3 mya–present). Periods of expansion generally—but not always—coincide with periods of increased mean evolutionary rates. Discretizing morphological change as primarily elaborative or innovative allows us to identify 260 that both processes happen at clade and species-level scales.

Averaging rates however, hides pulses of extreme rate variation (Fig.4). We identified pulses by isolating branches with at least twice the background evolutionary rate (mean scalar $r \geq 2$) that were shifted in at least 70% of the sampling posterior. Across all 19 focal traits, roughly 13% branches exhibited a significant rate pulse, with more than 3% 265 showing major shifts in evolutionary rate (mean scalar $r > 10$) (Fig.S14). Major shifts were primarily concentrated in head width, interlimb length, tail length and width, and upper arm length. In modules, nearly 16% of branches exhibited significant rate pulses, with 2% showing major shifts, concentrated in tail and body modules. Many rate increases are concentrated in the *Cyclodomorphus*–*Tiliqua* clade, with particularly rapid rates among

270 *Cyclodomorphus michaeli*, *casuarinae*, and *praealtus*. Body and tail traits also commonly show rate pulses in the crevice dwelling *Egernia stokesii* and *depressa* clades.

Simulations under uncorrelated and correlated Brownian Motion show differences in the accumulation of trait combinations. This highlights how evolution can be biased along particular axes (Fig.5, S5). Empirical traits generally conform to BM expectations, however 275 extreme phenotypes exceeding expectation have evolved in the feet of *Tiliqua* and tails of some *Egernia* (Fig.S9–S13).

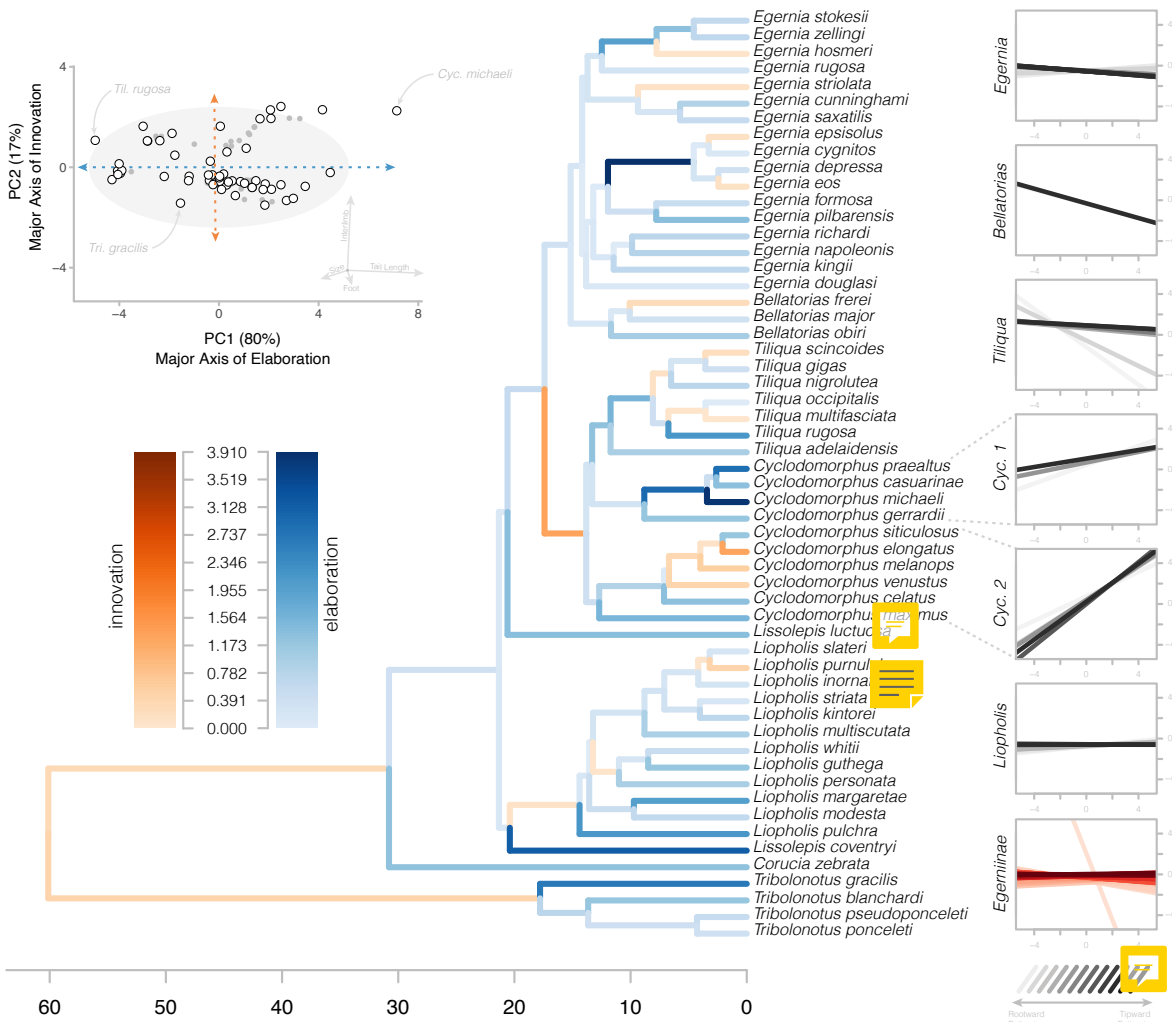


Figure 2: Major and minor axes of morphological change allow us to identify moments of elaboration (along PC1) and innovation (along PC2) in Egerniinae skinks. Top left—biplot of first two principal components show the distribution of observed species (white circles with black outlines) and estimated ancestors (grey circles) along the major axis of elaboration and innovation. Colored branches on the tree at center indicate the primary direction of morphological change from ancestor to descendant node. At right we visualize the varied relationships between these axes among groups. For each clade (genera and group as a whole) we plot the evolution of the relationship through time from the root of the clade (lightest regression) to the tips (darkest regression).

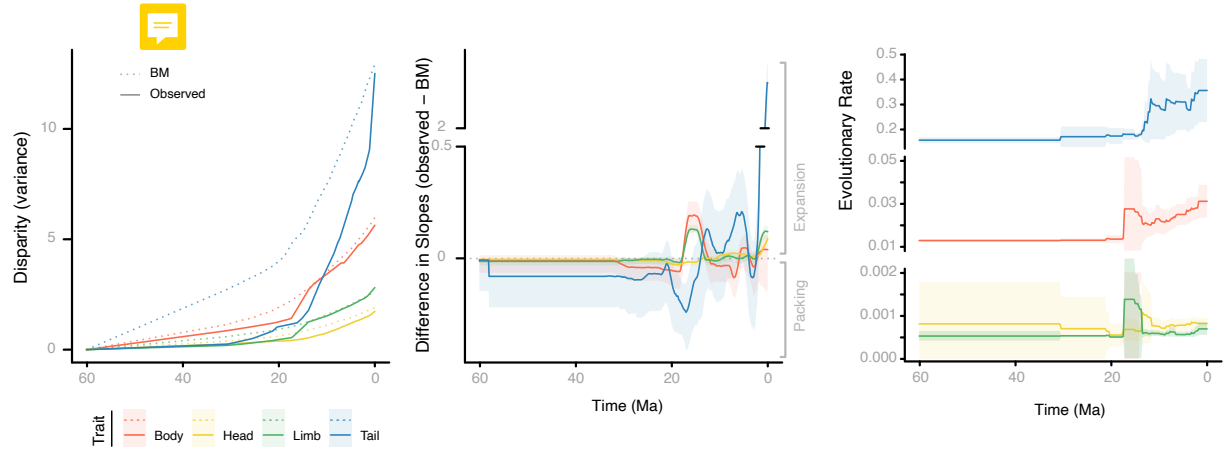


Figure 3: Evolutionary trajectories vary widely across modules and through time. (left) Accumulation of multivariate disparity (as variance) through time for each module (solid lines) compared to Brownian Motion (dotted lines). (center) The comparison of slopes of each module to BM highlights periods of morphological expansion (values greater than 0) and conservatism (values less than 0). (right) Evolutionary rates across modules are highly heterogeneous (see three different scales for y axis), showing periods of temporal variability, as well as high variances within modules and among traits (Fig.S15–S17).

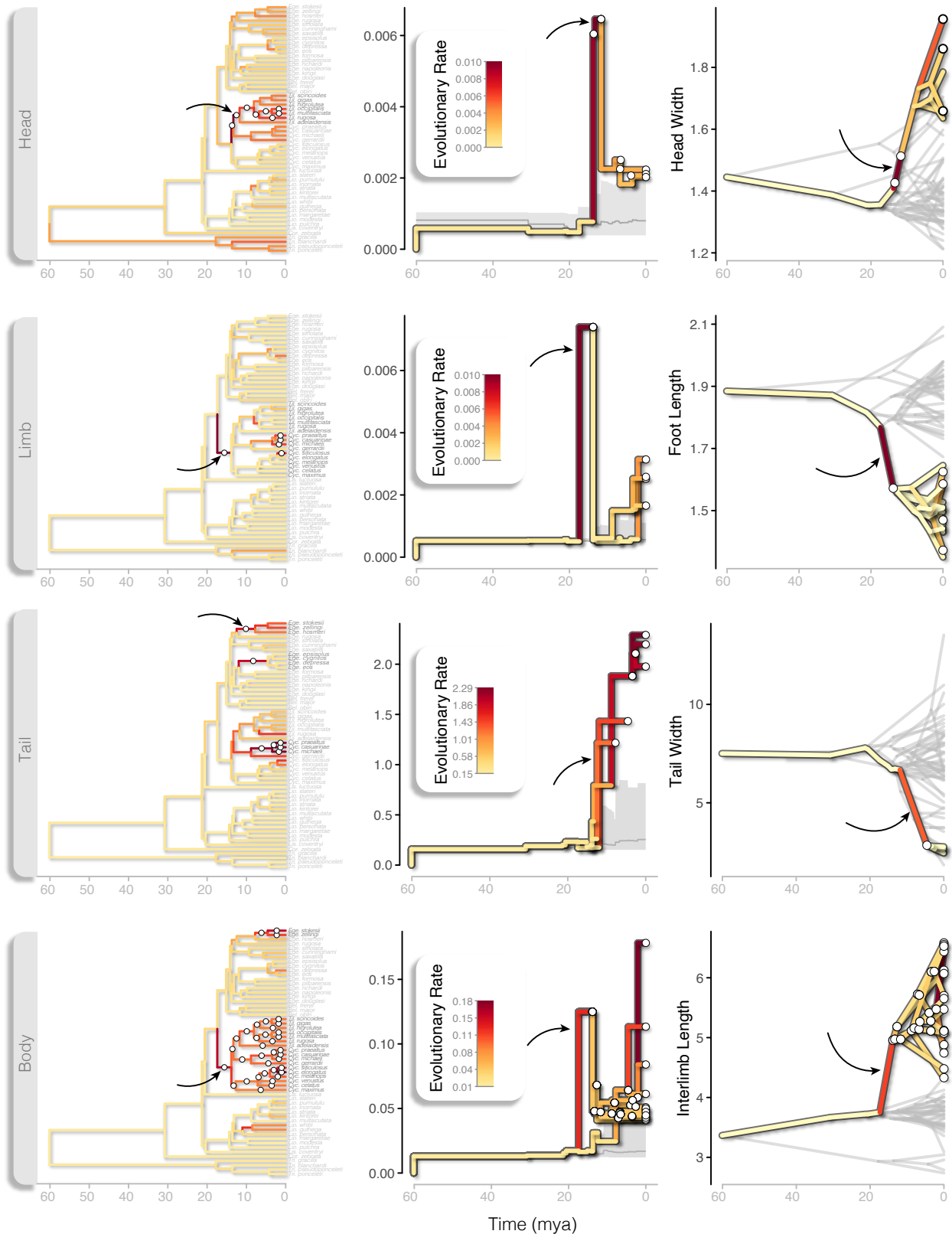


Figure 4: Rates caption below.

Figure 3.  Bursts in rates of phenotypic evolution are distributed across the egerniinae tree and exhibit strong departures from background rates. Rows represent morphological modules. In all plots branch colors correspond to estimated multivariate evolutionary rates, with significant rate changes noted by white circles at nodes or along branches. (left column) Egerniinae species trees highlighting the location of multivariate rate pulses. (center column) Branch rate trajectories plotted from the root node to nodes that show significant rate shifts. Solid grey envelope contains 95% quantiles of background evolutionary rates with the mean plotted in dark grey. (right column) Phenograms of an individual trait from each module showing the evolution of extreme phenotypes driven by bursts in evolutionary rate. In each row, a black arrow highlights a single branch of interest across all three plots.

280

285

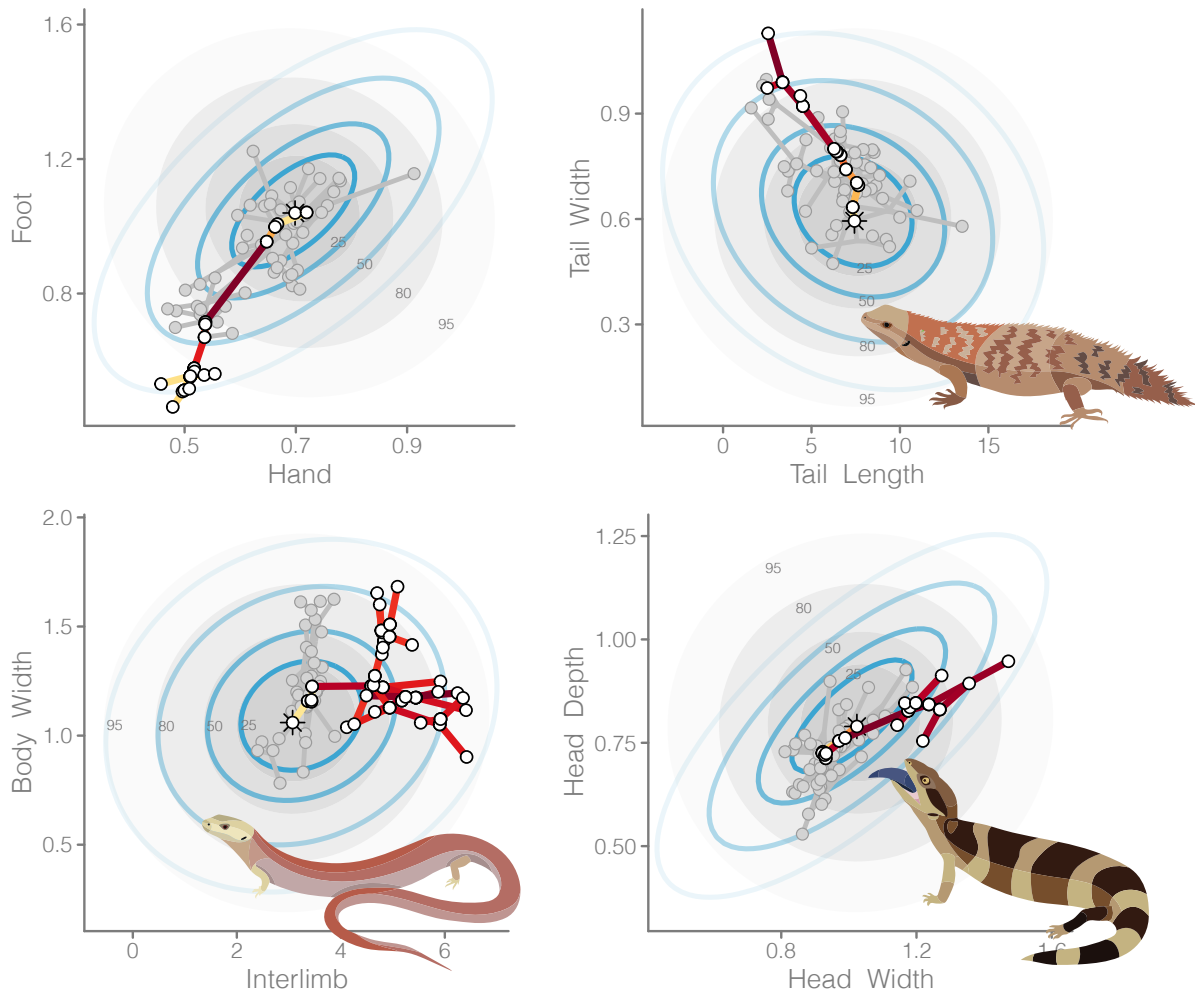


Figure 5: Novel morphologies exceed expectations of uncorrelated trait evolution. Bivariate plots show a phylomorphospace (species points connected by a phylogeny) of the Egerniinae. Each plot isolates a single clade within the group to highlight morphological extremes. Branches of the highlighted clade are colored according to evolutionary rates, with remaining species and branches in grey. In the background are ellipses containing 25/50/80/95% of traits simulated under empirical rates for uncorrelated (grey) and correlated (blue rings) Brownian Motion. Highlighted clades are (clockwise from top left: *Tiliqua*; *Egernia stokesii*–*E.hosmeri*, *Tiliqua rugosa*–*T.gigas*, *Cyclodomorphus*–*Tiliqua*). Thinking I should move the above figure to supplementary



Discussion

The variety of organismal forms has been a bottomless well of inspiration for scientists and the public, and an almost infinite source of data for macroevolutionary biologists to investigate the timing and accumulation of morphological diversity. Whether morphological disparity has accumulated early [CITE Foote 1997], uniformly [CITE Imfeld & Barker 2022], or via intermittent pulses [CITE Landis & Schraiber 2017; Deline et al. 2018] remains a contested topic at varied evolutionary scales. Here we investigate the morphological evolution

290

of the lizard body by looking across time, phylogeny, and body regions to better understand the modes by which traits evolve. We provide evidence for Egerniinae skinks that most traits evolve conservatively, but morphological novelty accumulates through extreme punctuations—jumps into new trait space. These jumps are relatively common, do not follow an established morphological order [CITE Salland & Friedman 2012], and can be nested to develop new trait combinations.

Phylogenomics of the Egerniinae

Skinks are a tremendously species rich group that make up more than 25% of all lizard diversity (1700+ species). The largest and most impressive skinks belong to the subfamily Egerniinae which are primarily distributed across Australia with a small number of species found in Indonesia, Papua New Guinea, and the Solomon Islands. Despite their importance as models of reptilian sociality [CITE Chapple 2003; Gardner et al. 2016] phylogenetic hypotheses for the Egerniinae have relied on a handful of molecular markers and limited species sampling [CITE Chapple et al. 2004; Chapple & Keogh 2006; Gardner et al. 2008]. Our exon capture dataset provides a well supported estimate of the relationships among all eight Egerniinae genera and 80% of described species. In agreement with previous estimates we recover the Egerniinae as members of the Lygosominae alongside the Sphenomorphinae, Eugongylinae, and Mabuyinae, suggesting an Asian origin for the subfamily [CITE Burbink et al. 2020].

Living egerniines are divided into three clades, comprising the enigmatic Crocodile Skinks *Tribolonotus*, the monotypic Solomon Islands endemic *Corucia*, and an Australian radiation. Splits among these groups are old (~60 & ~30 mya), and followed by the rapid Miocene divergence of all Australian Egerniinae genera (23–15 mya). These rapid speciation events result in short internal branches that prove difficult to resolve on a per-locus basis (Fig.1,S18). However, most of these difficult nodes are resolved by leveraging our 400 loci in ASTRAL, investigating summary statistics, and applying topology tests. Our new phylogenetic hypotheses of these nodes has necessitated that we propose taxonomic changes for two genera, which we provide in the attached Appendix. Some splits remain intractable however. The branching patterns among major *Egernia* clades, and the series of splits among *Lissolepis luctuosa*, *Liopholis*, and the remaining Australian egerniines have splits so short (300–400ky) that they exist at the limits of phylogenetic reconstruction. Regardless of resolution of these difficult branches, the radiation of Australian Egerniinae into divergent ecologies and morphologies happened rapidly and in concert across open landscapes, closed forests, deserts, and mountain peaks.

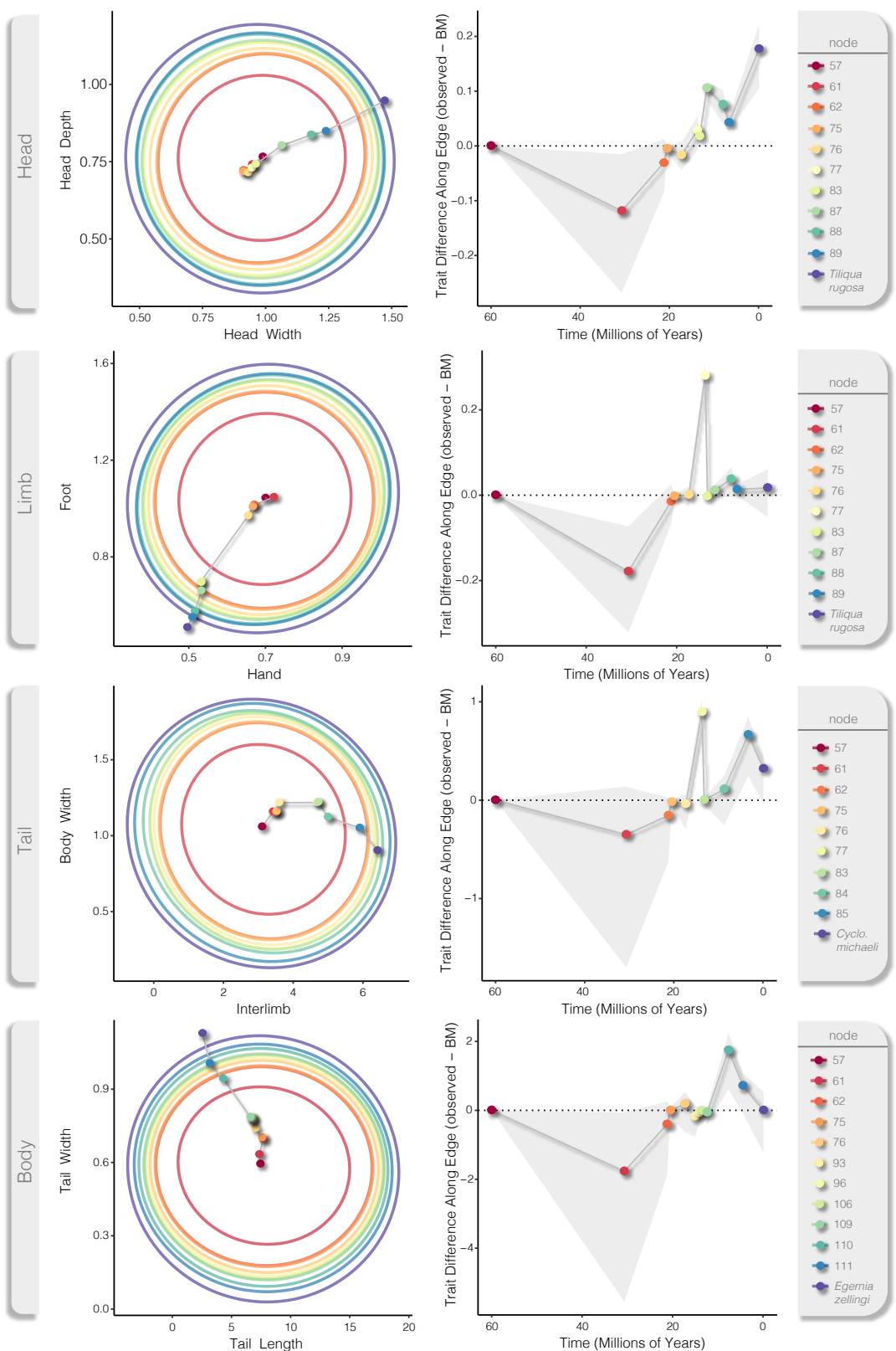


Figure 6: Phenotypic jumps caption below.

Figure 5. Phenotypic jumps are visible as greater than expected trait changes along branches, as estimated under the Variable Rates model and compared to Brownian Motion. Rows correspond to morphological modules, noted in grey at far left. Both circular and line plots show the evolutionary trajectory of focal traits from the root of the egerniine tree (node 57, dark red) to a single tip that has exhibited one or more rate bursts (dark purple). (left) Large colored circles represent the simulated distribution of trait values under Brownian Motion at each node along the root-to-tip trajectory. Small colored points represent observed and ancestral trait values as estimated under Variable Rates as they traverse the path root-to-tip connected by a grey line. (right) The line plot indicates the trait difference of nodes as (observed - simulated) values with 95% quantiles shown in light grey. Nodes that fall above the dotted line (0) show greater than expected trait change along the branch that leads to that node, visible as greater distances between points in the plots at left. Nodes falling below the dotted line show less trait change than expected.

340 Evolving Novel Phenotypes by Bursts

Earth's incredible biodiversity of forms and functions have evolved over hundreds of millions of years. Growing evidence suggests that much of this diversity accumulated via short periods of rapid phenotypic change, not by incremental divergence [CITE Uyeda et al.; Landis; Novack-Gotshall et al. 2022; Leslie et al. 2022 etc]. If this is true and pulsed morphological evolution is common, then it is important to understand how it contributes to the development of morphological novelty and diversity. To do this we identified how pulses are distributed through time, across the phylogeny, and among morphological axes.

Much of modern macroevolutionary thinking relies on Simpson's [1944] idea of adaptive zones. The varied adaptive landscape accumulates diversity as lineages traverse into new adaptive zones that are centered around fitness peaks. Lineages move into new zones by evolutionary jumps—rapid movement across suboptimal space. In comparative studies the idea of a multipeak morphological landscape is often described by multi-optima OU models [CITE Hansen; OUwie; Burin et al. 2023]. While these models account for the clustering of species around discrete trait values (evolutionary ‘clumpiness’) they do not explain well the process of movement across the landscape to occupy new peaks. Our analysis of the lizard body plan provides evidence that pulses in evolutionary rate and coincident phenotypic change are common across many morphological traits (preferred in 13 of 19 traits). This suggests that large distances of suboptimal trait space can be quickly traversed to reach new morphological realms. However, the accumulation of morphological disparity does not appear to be dictated solely by rare jumps, or to occur explicitly at speciation, as in the punctuated equilibrium model of Eldredge & Gould (1972). Instead, we find broad support for a model in which the background process of evolution by a random walk (Brownian Motion) is punctuated by bursts in evolution that result in jumps to new adaptive zones. When comparing modeled empirical data to simulations, these jumps are observable as large trait changes along individual branches (Fig.6). This heterogeneous mode facilitates the evolution of novel and divergent morphologies (Fig.4) from among a general morphological diffusion process. In this way we attempt to find common ground for Darwinian and Simpsonian evolution.

In the Variable Rates model branch-specific shifts are indicative of an increase in evolutionary rate but remain a parameter of a random walk (Brownian) process. So, increasing the evolutionary rate suggests an increase in the *evolvability* and ultimately the potential

variance of a lineage. An alternative interpretation for the identification of bursts could instead be a directional trend towards distinct trait values. A recently designed method for addressing this—the *fabric* model of *BayesTraits V4*—proposes that excess rate estimates
375 could instead be absorbed by a biased walk to new trait space. Importantly, this does not fundamentally change the outcome that evolution has swerved into a new morphological lane, but it does suggest a difference in the evolutionary mode. Whereas a rate pulse suggests a rapid, random exploration of trait space that lands in a new zone, directional trends elicit a guided evolutionary walk towards a new area of trait space. Because a guided walk is
380 directional the evolutionary rate need not be rapid. Regardless, the jump in trait value along a branch, and evolution of a new phenotype remains the same. This provides an appealing explanation for scenarios where selection might be particularly effective, such as in small populations or those with high trait variances.                                     <img alt="green square icon" data-bbox="515 7738 5

tional morphologies are rare. In a few cases, such as the feet of some *Tiliqua* and the tails of some *Egernia*, contemporary trait values fall outside what we expect under a uncorrelated random walk model. These instances provide the strongest cases for active selection driving
420 the evolution of phenotypes (Fig.5).

Conclusions

Animal bodies are made up of anatomical regions which act in concert to perform necessary functions. But the evolution of these regions does not necessarily occur in concert, resulting in the amazing morphological diversity we see across animals. Instead, individual morphological traits and the modules they comprise often evolve heterogeneously. This heterogeneity
425 commonly takes the form of rapid phenotypic divergence that results in novel phenotypes. We suggest that these evolutionary discontinuities are prevalent in Egerniinae skinks and likely a common process in morphological diversification across animals. **Probably needs a sentence or two more about general application of these ideas.**

430 **Appendix**

Taxonomic Implications and Changes

As a result of our phylogenetic investigation, some taxonomic issues must be addressed and others will unfortunately remain outstanding until more focused sampling can be achieved.

We comment on both cases below. **The order of the following comments can easily be shifted**

435 (1) Paraphyly of *Lissolepis*: Phylogenetic estimation and topology testing do not support the monophyly of *Lissolepis*. The type species of *Lissolepis* is *L.luctuosa* (Peters 1866), and despite *L.coventryi* (Storr 1978) forming a clade with *Liopholis*, these taxa are morphologically distinct. We feel that to acknowledge the distinctiveness of *L.coventryi* the best course of action is to erect a new genus to contain this species.

Paluarius gen. nov. Brennan ...

Egernia Storr 1978

Lissolepis Gardner 2008

440 445 Type species: *Egernia coventryi* Storr 1978

Diagnosis and definition: Currently a monotypic genus comprising a single medium sized ($\bar{x} = 80$ mm; max = 100 mm) skink with four well developed limbs each with five digits and fourth toe much longer than third. Lower eyelid movable and without a transparent ‘window’. Parietal and nasal scales both narrowly separated. Ear aperture small and with two anterior lobules. Distinguished from *Lissolepis* by broad geographic separation (southwest WA for *Lis.*; extreme southeast SA and coastal VIC for *Pal.*), continuous striped (*Paluarius*) rather than spotty (*Lissolepis*) dorsal patterning, shorter and blunter head (head length 15% of SVL in *Pal.*, 20% in *Lis.*), fewer midbody scale rows, longer postnasal crease that runs to the top of the nasal scale, and smaller size (80–100 mm vs. 100–129mm).

450 455 Etymology: This skink lives among swamps, heaths, and marshes in far southeastern Australia. In allusion to its preferred habitat, from latin ‘palus’—swamp and ‘-arius’—where things are kept, together meaning ‘keeper of the swamp’.

Contents: *Paluarius coventryi* comb. nov. (Storr 1978)

460 (2) Paraphyly of *Cyclodomorphus*: Phylogenetic estimates and topology testing do not support the monophyly of *Cyclodomorphus* (). The type species of *Cyclodomorphus* is *C. casuarinae* (Dumeril & Bibron 1839), which along with the species *gerrardii*, *michaeli*, and *praealtus* form a clade with *Tiliqua*. We propose a new generic name to contain the taxa more closely related to *C. maximus* than to *C. gerrardii*.

465 *Caeruleulus* gen. nov. Brennan ...

Cyclodus Dumeril & Bibron 1839

Hinula Gunther 1867

Lygosoma

Tiliqua

470 *Omolepida* Gray 1845

Cyclodomorphus Fitzinger 1843

Type species: *Omolepida maxima* Storr 1976

Diagnosis and definition: A genus of moderate to large, elongate skinks characterized by long interlimb (trunk) lengths and relatively short limbs, each with five digits. Many
475 scalation characters are shared with *Cyclodomorphus*, and so make distinguishing the two difficult. Starting from the snout, nasals are in contact with one another and broadly contact the frontonasal which widely separates the prefrontals. There are no subocular scales, but three supraocular scales, the anterior two of which contact the frontal. Eyelid movable and no transparent ‘window’. Parietal scales are widely separated by an interparietal scale. Ear
480 opening small, with small anterior lobules (usually 2).

Etymology: From the Latin ‘caeruleus’ for blue and the diminutive ‘-ulus’, meaning ‘little blue one’, alluding to their blue tongues and smaller size relative to the larger ‘bluetongue’ relatives *Tiliqua*.

Contents: *Caeruleulus branchialis* comb. nov. (Gunther 1867); *Caeruleulus celatus* comb.
485 nov. (Shea & Miller 1995); *Caeruleulus maximus* comb. nov. (Storr 1976); *Caeruleulus melanops elongatus* comb. nov. (Shea & Miller 1995); *Caeruleulus melanops melanops* comb. nov. (Stirling & Zietz 1893); *Caeruleulus melanops siticulosus* comb. nov. (Shea & Miller 1995); *Caeruleulus venustus* comb. nov. (Shea & Miller 1995).

Comment: Wells (2007) proposed splitting *Cyclodomorphus*, reallocating *C. gerrardii* to
490 *Hemisphaeriodon* and creating a new generic name for the *Cyclodomorphus maximus* clade. In following the best practices in herpetological nomenclature outlined by Kaiser et al. (2013) and adopted by the Australian Society of Herpetologists in their Position Statement on Taxonomy (2022) we do not recognize the name proposed by Wells (2007) and instead provide *Caeruleulus* as the generic name for this clade of egerniine skinks.

495 (3) *Cyclodomorphous melanops*: Our limited sampling suggests species-level divergences among the three subspecies of *C. melanops* (~4mya, 2mya), however unpublished mtDNA data shows more complicated genetic history among these taxa and the closely related *C. venustus*, *C. celatus*, and the currently unsampled *C. branchialis*. In light of these results
500 we take the conservative stance of retaining the subspecies as is, and suggest a more focused study with greater sampling would provide better understanding of this morphologically conservative clade.

(4) *Egernia stokesii*: Similarly, the divergence between *E. stokesii* subspecies *E.s.badia* and *E.s.zellingi* are comparatively deep (~4.5mya), and subspecies are recovered as reciprocally monophyletic. However, our sampling lacks representatives of the nominate subspecies *E.s.stokesii*. Unpublished mtDNA data does not appear to distinguish between subspecies *E.s.stokesii* and *E.s.badia*, and so we refrain from making taxonomic changes without having *E.s.stokesii* included in our analyses.

510 (5) Paraphyly of *Liopholis inornata*: Our sampling of *L. inornata* and sister taxa *L. slateri* and *L. sp. nov.* from Purnululu highlight a complicated phylogenetic history. As currently understood, *L. inornata* is a wide ranging species found across much of arid WA, SA, NSW, and QLD. This range overlaps entirely with *L. slateri* with which it could potentially
515 be confused, but remains allopatric from *L. sp. nov.* Purnululu. We highlight this clade as a group which needs a much more thorough population genetic assessment to resolve.

Supplementary Material

Supplementary material included below consists of additional figures, tables, and extended
520 methods to complement the main text.

Table S1. Taxon sampling for this project.

Genus	Species	Subspecies	Specimen Registration	ABTC No.	Locality	State	Country	Latitude	Longitude
Bellatorias	<i>frerei</i>	—	AMS R.113970	10881	Bunya Mountains	QLD	Australia	-	-
Bellatorias	<i>frerei</i>	—	AMS R.96317	11439	Heathlands	QLD	Australia	-	-
Bellatorias	<i>major</i>	—	SAMA R.33412	4115	Whian Whian SF	NSW	Australia	-	-
Bellatorias	<i>obiri</i>	—	AMS R.100018	11440	Jabiluka	NT	Australia	-	-
Corucia	<i>zebrata</i>	—	—	50418	Levaleva Choiseul Island	—	Solomon Islands	-	-
Cyclodomorphus	<i>melanops</i>	<i>elongatus</i>	MAGNT R20662	29403	Finke Gorge NP	NT	Australia	-	-
Cyclodomorphus	<i>casuarinae</i>	—	SAMA R.22957	54924	Mount Victoria	TAS	Australia	-	-
Cyclodomorphus	<i>celatus</i>	—	SAMA R.63333	101476	—	WA	Australia	-	-
Cyclodomorphus	<i>gerrardi</i>	—	SAMA R.22873	54920	Burns Beach	WA	Australia	-	-
Cyclodomorphus	<i>maximus</i>	—	SAMA R.34884	16792	Paluma	QLD	Australia	-	-
Cyclodomorphus	<i>melanops</i>	<i>siticulosus</i>	WAM R168816	135574	Middle Osborn Island	WA	Australia	-	-
Cyclodomorphus	<i>melanops</i>	—	SAMA R.52374	58905	St. Francis Island	SA	Australia	-	-
Cyclodomorphus	<i>praelectus</i>	—	SAMA R.34056	11739	Mount Stuart Homestead	WA	Australia	-	-
Cyclodomorphus	<i>venustus</i>	—	—	97283	Bogong High Plains	VIC	Australia	-	-
Egernia	<i>cunninghami</i>	—	SAMA R.18869	54897	Port Germein Dump	SA	Australia	-	-
Egernia	<i>cunninghami</i>	—	AMS R.112873	11398	Yetman	NSW	Australia	-	-
Egernia	<i>depressa</i>	—	AMS R.118939	14392	Kanangra Walls	NSW	Australia	-	-
Egernia	<i>depressa</i>	—	SAMA R.22856	53933	Python Pool	WA	Australia	-	-
Egernia	<i>douglasi</i>	—	WAM R120631	63425	Mardathuna	WA	Australia	-	-
Egernia	<i>eos</i>	—	ABTC 141482	141482	Beverley Springs Homestead	WA	Australia	-	-
Egernia	<i>episolus</i>	—	WAM F98079	23913	Ainsley Gorge	WA	Australia	-	-
Egernia	<i>formosa</i>	—	WAM F90897	63515	Woodstock	WA	Australia	-	-
Egernia	<i>formosa</i>	—	SAMA R.29267	53997	Yalgoo	WA	Australia	-	-
Egernia	<i>hosmeri</i>	—	WAM F103993	611869	Woodstock Station	WA	Australia	-	-
Egernia	<i>kingii</i>	—	SAMA R.36707	17065	Mount Isa	QLD	Australia	-	-
Egernia	<i>napoleonis</i>	—	SAMA R.29444	54006	Mount Clarence	WA	Australia	-	-
Egernia	<i>pilleensis</i>	—	SAMA R.23080	53949	Dennmark	WA	Australia	-	-
Egernia	<i>richardi</i>	—	WAM R1.32519	63479	Burrup Peninsula	WA	Australia	-	-
Egernia	<i>richardi</i>	—	SAMA R.26315	40639	Koonalda Station	SA	Australia	-	-
Egernia	<i>rugosa</i>	—	SAMA R.63272	112886	Merderyrah Sandpatch	SA	Australia	-	-
Egernia	<i>rugosa</i>	—	—	108820	Charleville	QLD	Australia	-	-
Egernia	<i>saxatilis</i>	<i>intermedia</i>	SAMA R.44004	12812	Charleville	QLD	Australia	-	-
Egernia	<i>stokesii</i>	<i>zellingi</i>	SAMA R.42897	9143	The Grampians	VIC	Australia	-	-
Egernia	<i>stokesii</i>	<i>zellingi</i>	SAMA R.45053	35026	Stonehenge	QLD	Australia	-	-
Egernia	<i>stokesii</i>	<i>zellingi</i>	SAMA R.44127	57871	Toopawarina Hill	SA	Australia	-	-
Egernia	<i>stokesii</i>	<i>badia</i>	WAM R.135193	63511	Pernatty Station	SA	Australia	-	-
Egernia	<i>stokesii</i>	<i>badia</i>	WAM R152997	63511	Walycatchem	WA	Australia	-	-
Egernia	<i>stokesii</i>	<i>badia</i>	WAM R152998	92933	Waiga Rock	WA	Australia	-	-
Egernia	<i>striolata</i>	—	AMS R.126116	92934	Waiga Rock	WA	Australia	-	-
Egernia	<i>striolata</i>	—	SAMA R.53262	1150	Denham	NSW	Australia	-	-
Egernia	<i>striolata</i>	—	SAMA R.55661	70470	Telowie	SA	Australia	-	-
Egernia	<i>QM_J86594</i>	—	Moorrinya NP	76988	Moorrinya NP	QLD	Australia	-	-
Egernia	<i>QM_R38916</i>	—	Durkai SF	100573	Durkai SF	QLD	Australia	-	-
Eutropis	<i>longicaudata</i>	—	57273	—	—	—	Malaysia	-	-

Genus	Species	Subspecies	Specimen Registration	ABTC No.	Locality	State	Country	Latitude	Longitude
<i>Liopholis</i>	<i>guthega</i>	—	SAMA R37781	16273	Kosciusko NP	NSW	Australia		
<i>Liopholis</i>	<i>inornata</i>	—	MAGNT R20673	29437	Finke Gorge NP	NT	Australia		
<i>Liopholis</i>	<i>inornata</i>	—	SAMA R45219	58081	Mootatunga	SA	Australia		
<i>Liopholis</i>	<i>inornata</i>	—	SAMA R49140	58604	Eyre Peninsula	SA	Australia		
<i>Liopholis</i>	<i>inornata</i>	—	NMV D65868	61607	Buninyonia Springs	WA	Australia		
<i>Liopholis</i>	<i>kintorei</i>	—	WAM R131047	63449	—	WA	Australia		
<i>Liopholis</i>	<i>margaretae</i>	—	SAMA R51590	42404	Annata	SA	Australia		
<i>Liopholis</i>	<i>margaretae</i>	—	SAMA R24815	53965	Mount Remarkable NP	SA	Australia		
<i>Liopholis</i>	<i>modesta</i>	—	SAMA R39172	12411	Retreat	NSW	Australia		
<i>Liopholis</i>	<i>montana</i>	—	SAMA R37768	16389	Mount Gingera	ACT	Australia		
<i>Liopholis</i>	<i>multiscutata</i>	—	SAMA R63458	126142	—	SA	Australia		
<i>Liopholis</i>	<i>pulchra</i>	—	WAM R132054	63464	D'Entrecasteaux NP	WA	Australia		
<i>Liopholis</i>	<i>sp. nov.</i>	—	WAM R156715	85105	Purnululu NP	WA	Australia		
<i>Liopholis</i>	<i>slateri</i>	—	—	99920	Finke River	NT	Australia		
<i>Liopholis</i>	<i>striata</i>	—	SAMA R45402	58180	Anpeinna Hills	SA	Australia		
<i>Liopholis</i>	<i>whitii</i>	—	SAMA R53588	94846	Spring Mount	SA	Australia		
<i>Lissolepis</i>	<i>coventryi</i>	—	SAMA R45916	58241	Nelson	SA	Australia		
<i>Lissolepis</i>	<i>luctuosa</i>	—	WAM R90386	135575	Walpole	WA	Australia		
<i>Lissolepis</i>	<i>luctuosa</i>	—	WAM R90226	135576	Lake Wilson	WA	Australia		
<i>Tiliqua</i>	<i>adelaidensis</i>	—	SAMA R42426	57682	Burra	SA	Australia		
<i>Tiliqua</i>	<i>gigas</i>	—	AMS R.124720	48811	Usino	Manus	Papua New Guinea		
<i>Tiliqua</i>	<i>gigas</i>	—	AMS R.124720	48812	Usino	Manus	Papua New Guinea		
<i>Tiliqua</i>	<i>multifasciata</i>	—	AMIS R.129710	50170	Gulegule Normanby Island	Milne Bay	Papua New Guinea		
<i>Tiliqua</i>	<i>nigrolutea</i>	—	SAMA R49974	37896	Purni Bore	SA	Australia		
<i>Tiliqua</i>	<i>occipitalis</i>	—	SAMA R33410	4114	Clarkefield	VIC	Australia		
<i>Tiliqua</i>	<i>rugosa</i>	—	SAMA R28391	54961	Iron Knob	SA	Australia		
<i>Tiliqua</i>	<i>rugosa</i>	—	SAMA R18978	55216	Bremer Bay	WA	Australia		
<i>Tiliqua</i>	<i>scincoides</i>	intermedia	SAMA R20587	55264	Cowell	SA	Australia		
<i>Tiliqua</i>	<i>scincoides</i>	intermedia	QM J51107	24812	Cape Flattery	QLD	Australia		
<i>Tiliqua</i>	<i>scincoides</i>	—	WAM R112258	101416	Latdalam	—	Indonesia		
<i>Tiliqua</i>	<i>scincoides</i>	—	SAMA R28511	54968	Minnipa	SA	Australia		
<i>Tiliqua</i>	<i>gracilis</i>	—	SAMA R53937	70143	Tunnel Creek Gorge	WA	Australia		
<i>Tribolonotus</i>		—	AMIS R.122119	14359	Karkar Island	—	Papua New Guinea		

Table S2. Fossil calibrations as implemented in MCMCTree. The root (Mabuyinae + Egerniinae) and the Egerniinae crown are calibrated with Cauchy distributions based on estimates from previous studies. These leave 2.5% of the distribution each above and below the minimum and maximum ages noted below. The calibration for the crown of Australian Egerniinae is bounded on the lower end by the Dworman Local Fauna of Riversleigh which includes *Tiliqua pusilla* and *Egernia gillespieae*, and on the upper end by *Proegernia palankarinensis* and *P. mikebulii*. The prior allows 2.5% below the minimum bound and 20% above the maximum bound. The remaining calibrations are all soft minimums with 2.5% below the minimum.

Node	Fossil Information	Calibration	Split	Source
A	Soft Secondary	'>0.5<0.8'	Root (Mabuyinae + Egerniinae)	[CITE Burbink et al. 2021; Thorn et al. 2021]
B	Soft Secondary	'>0.37<0.62'	Crown Egerniinae (<i>Tribolonusotus</i> + all others)	[CITE Thorn et al. 2019; Thorn et al. 2021]
C	<i>Tiliqua pusilla</i> [†] , <i>Egernia gillespieae</i> [†] , <i>Proegernia palankarinensis</i> [†] , <i>P. mikebulii</i> [†]	'B(0.15,0.26,0.025,0.2)' (Corucia + all others)	Crown Australian Egerniinae (Corucia + all others)	[CITE Martin et al. 2004; Thorn et al. 2019]
D	<i>Egernia gillespieae</i> [†]	'>0.15'	Crown <i>Egernia</i>	[CITE Thorn et al. 2019]
E	<i>Tiliqua cf. scincoides</i> [†]	'>0.36'	<i>Tiliqua gigas</i> + <i>Tiliqua scincoides</i>	[CITE Mackness & Hutchinson 2000]
F	<i>Egernia cf. hosmeri</i> [†]	'>0.36'	<i>Egernia hosmeri</i> + <i>Egernia stokesii</i>	[CITE Mackness & Hutchinson 2000]

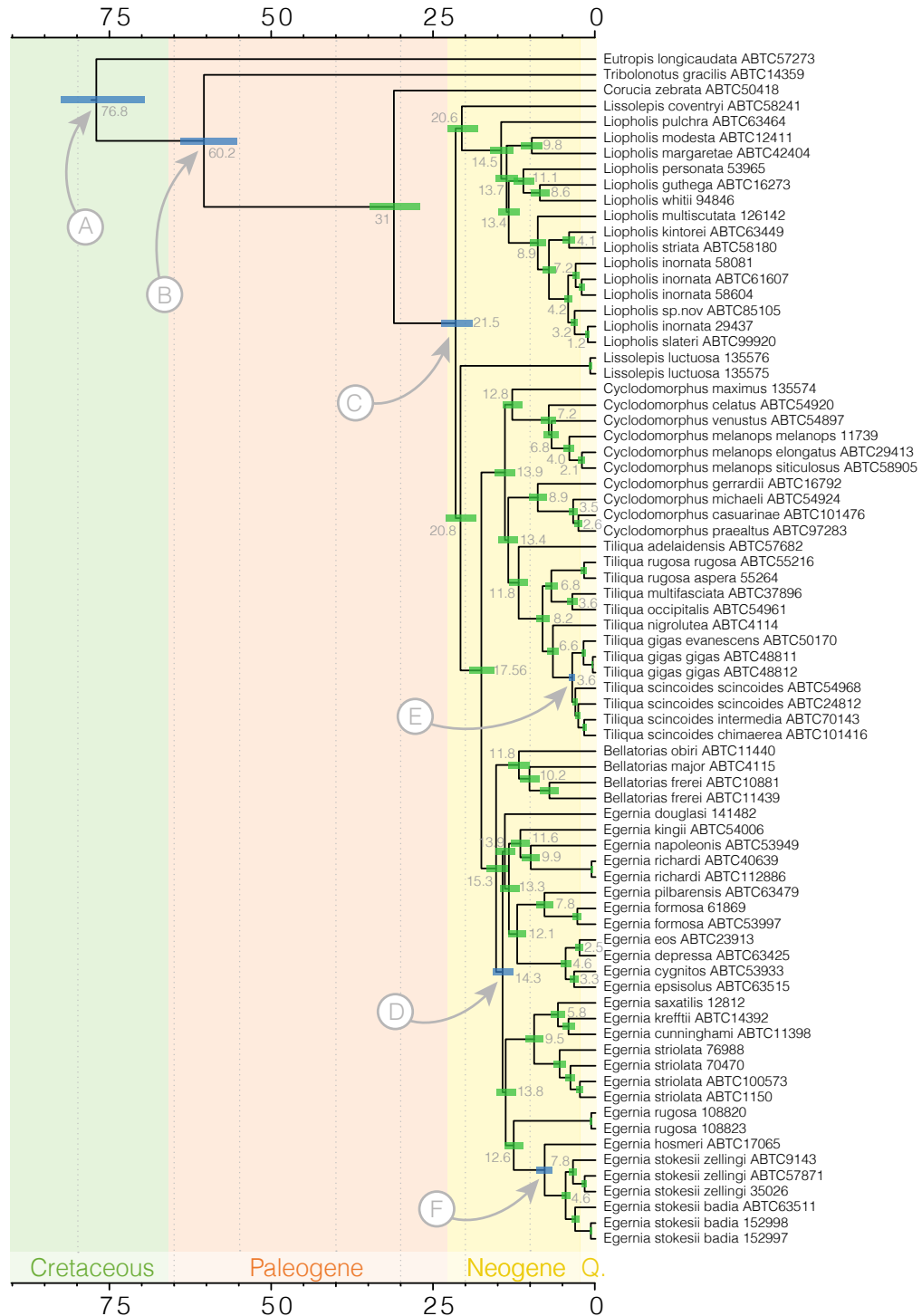


Figure S1: Egerniinae species tree estimated with ASTRAL from IQTREE genetrees and time-calibrated with MCMCTree. Shaded bars at nodes indicate 95% confidence estimates on ages. Nodes labelled by letters A–F correspond to fossil calibrations listed in Table S2.

Alignment Specifications

Input MAFFT/MUSCLE alignments were refined with MACSE using the following call:

```
$ java -jar /Applications/macse_v2.03.jar \
    -prog refineAlignment -align [rough alignment path] \
    -optim 1 -local_realign_init 0.1 -local_realign_dec 0.1 \
    -fs 10 -stop 10
```

530 Investigating Data Completeness and Informativeness

Below we visualize data completeness and informativeness on a per sample and per locus basis, as well as provide some insight into our data cleaning and sample selection.

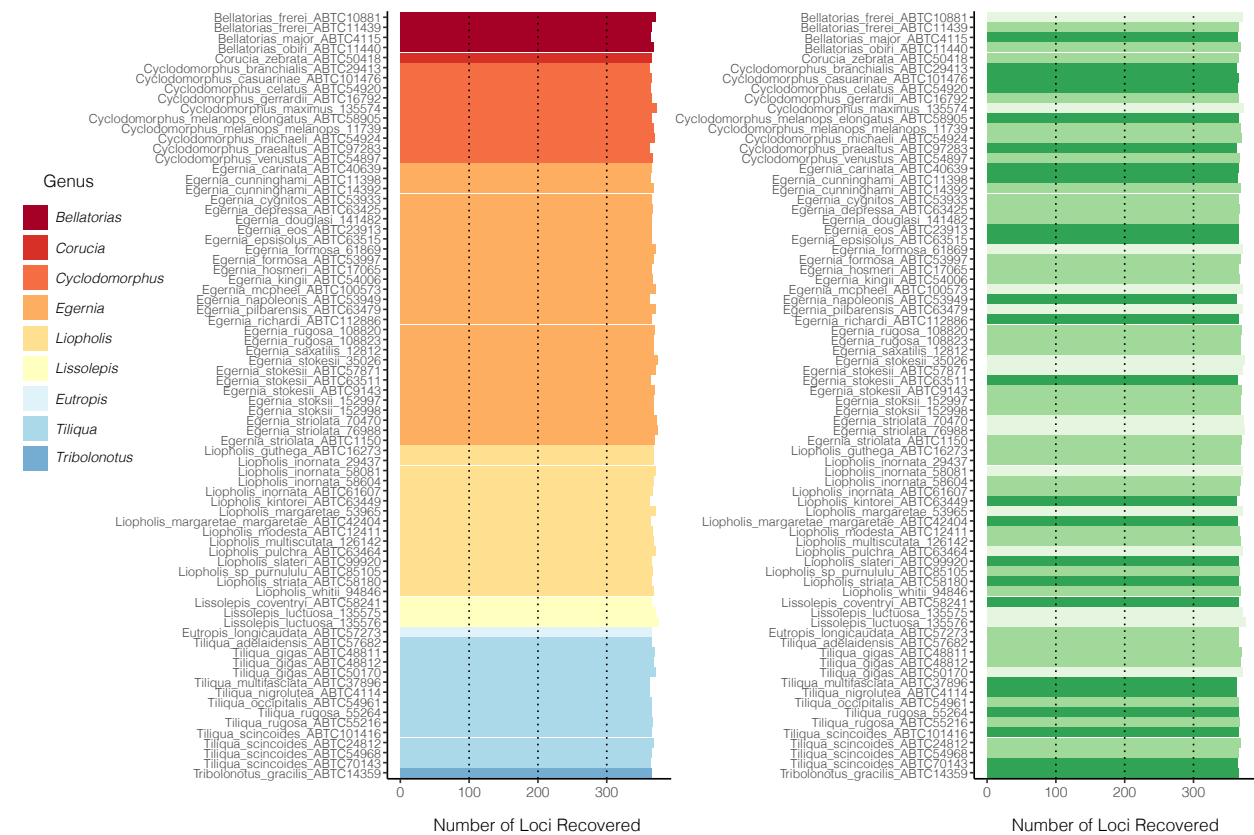


Figure S2: Number of loci recovered per sample for all egerniinae and outgroup taxa included in the molecular data. Samples are colored by Genus (left) and coverage (right).

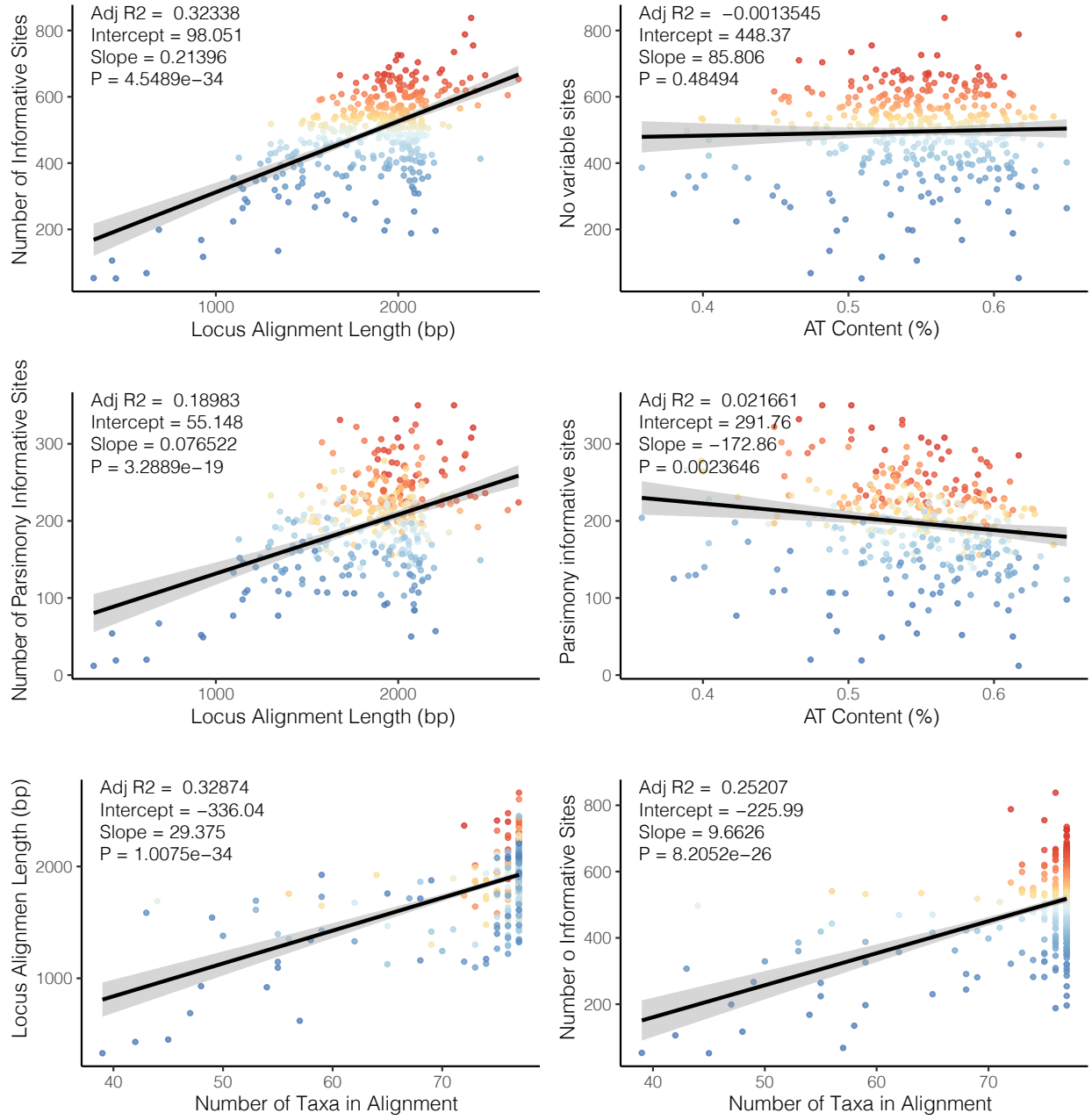


Figure S3: Plots of individual locus completeness and informativeness. Points are colored according to number of informative (variable) sites (blue—few, red—many). Top row shows the number of variable sites in each alignment as a function of alignment length and AT content. The middle row shows the number of parsimony informative sites as a function of alignment length and AT content. The bottom row shows alignment length and number of variable sites as a function of completeness.

Morphological Measurements

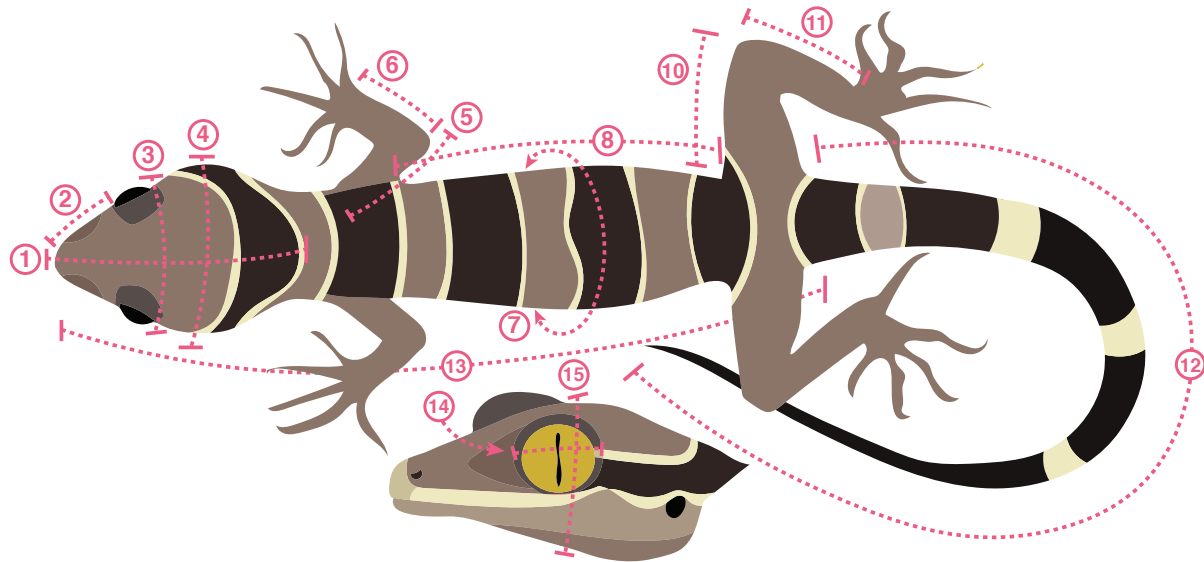


Figure S4: The 21 linear measurements collected.

Initial morphological measurements used for data investigation:

Measurement	Abbreviation	Method
Snout-vent length	SVL	From the tip of the snout to the vent.
Snout-axilla length	SAL	From the tip of the snout to the midpoint of the crease between the fore-limb and the body on the ventral surface.
Inter-limb length	ILL	Midpoint of the crease on the ventral surface where the fore-limb connects to the body, to the midpoint of the crease on the ventral surface where the hind-limb connects to the body.
Body width	BW	From one lateral side of the body to the other, where possible at the midpoint of the ILL.
Pelvic width	PW	From the midpoint of the crease on the ventral surface where the left hind limb connects to the body, to the midpoint of the crease on the ventral surface where the right hind limb connects to the body.
Pelvic height	PH	From the top of the dorsal surface where the PW was measured, to the bottom of the ventral surface where the PW was measured.
Head width	HW	Widest part of the head from one dorsal-lateral edge to the other edge.

Measurement	Abbreviation	Method
Head length	HL	From the nose tip, to the anterior of the ear.
Snout length	SN	From the nasal opening to the anterior of the eye.
Eye diameter	ED	From one side of the eye to the other.
Head depth	HD	From the top of the tallest part of the head on the dorsal surface, to the bottom of the ventral surface under the jaw.
Tail width	TW	Measured at the vent, from one dorsal-lateral edge to the other edge.
Fore-limb length	FLL	Measured fully extended from the midpoint of the crease on the ventral surface where the front limb connects to the body, to the end of longest toe (claw included).
Front foot	FFOOT	From the base of the foot to the end of the longest toe (claw included).
Lower front limb	LFL	Measured from the base of the lower fore limb to the juncture where the limb meets the front foot.
Upper front limb	UFL	Measured from the crease on the ventral surface where the fore limb connects to the body, to the end of the lower front limb.
Hind-limb length	HLL	From the midpoint of the crease on the ventral surface where the hind limb connects to the body, to the end of longest toe (claw included)
Hind foot	HFOOT	From the base of the hind foot to the end of the longest toe (claw included)
Lower hind limb	LHL	Measured from the top of the knee joint to the heel juncture where the limb meets the front foot.
Upper hind limb	UHL	Measured from the crease on the ventral surface where the hind limb connects to the body, to the end of the knee.

535 Final morphological traits used for phenotypic analyses:

Measurement	Shorthand	Method
Interlimb length	Interlimb	see above
Body width	Body_Width	see above
Pelvic width	Pelvic_Width	see above
Pelvic height	Pelvic_Height	see above
Head width	Head_Width	see above
Snout length	Snout_Eye	see above
Eye diameter	Eye_Diameter	see above
Head depth	Head_Depth	see above

Measurement	Shorthand	Method
Tail width	Tail_Width	see above
Tail length	Tail_Length	see above
Upper front limb	Upper_Arm	see above
Lower front limb	Lower_Arm	see above
front foot	Hand	see above
Upper hind limb	Upper_Leg	see above
Lower hind limb	Lower_Leg	see above
Hind foot	Foot	see above
Neck length	Neck	Snout_Axilla - Head_Length
Posterior skull	Pos_Skull	Head_Length - (Snout_Eye + Eye_Diameter)
Pelvic gap	Pelvic_Gap	Snout_Vent - (Interlimb + Snout_Axilla)

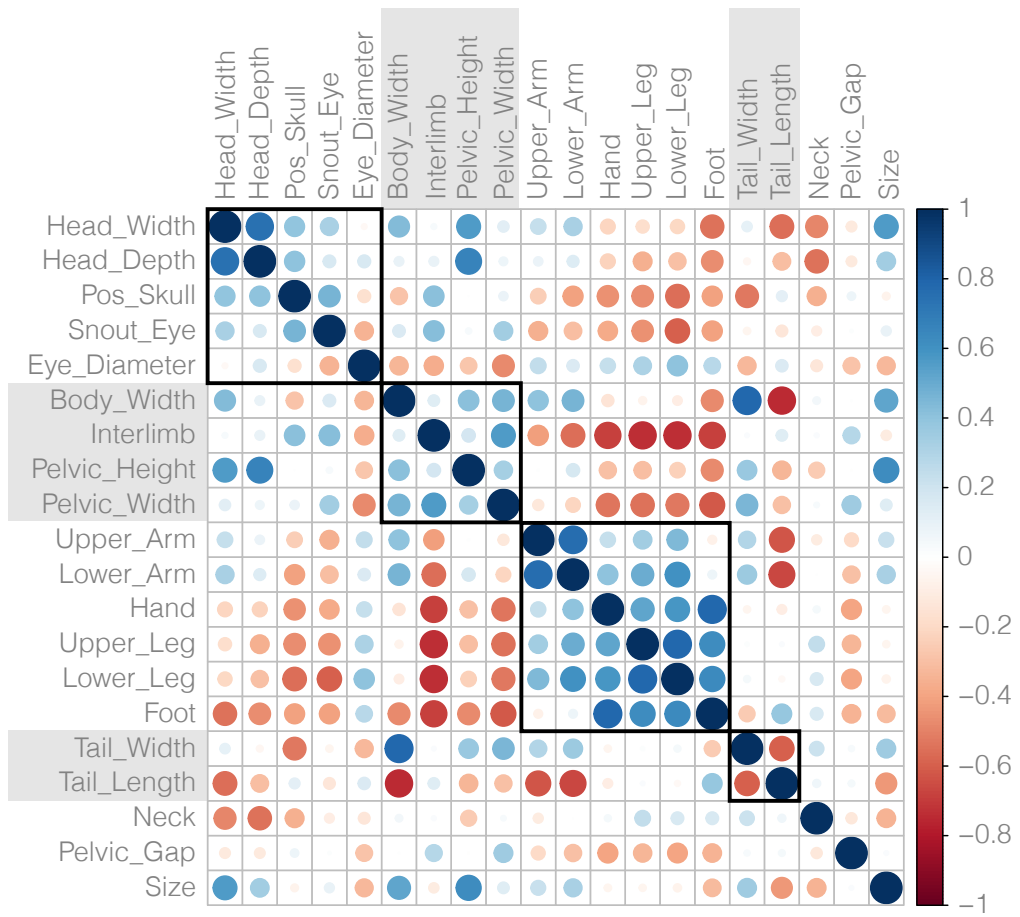


Figure S5: Correlation plot of all morphological traits after removing size via log-shape ratios. Some traits retain strong correlations despite removing the effect of size. Traits are organized according to the morphological module they belong to. Plot generated using *corrplot* [Wei & Simko 2021].

Modelling Trait Evolution and Disparity

We started by generating mean trait values per species. To remove the effect of size on individual traits (allometry) we then calculated the geometric mean of all traits by species and used this to transform trait measurements into log-shape ratios. This also provided
540 an additional trait *size*. To investigate integrated and modular evolution we estimated correlations among traits and provided this as input for the package *EMMLi* [CITE Goswami & Finarelli]. *EMMLi* also requires *a priori* hypotheses of the assignment of traits to modules. We provided five general hypotheses for model comparison with the most specialized model allowing traits of the head, limbs, body, and tail to evolve as independent modules, and the
545 most restrictive null model lumping all traits into a single module. *EMMLi* also allowed us to compare models in which the correlation coefficient among modules and among traits within modules is either similar or different (see Goswami & Finarelli Fig.2). Once we established the preferred model (head, body, limbs, tail as separate modules with differing inter- and intramodule correlations) we split our traits into module-specific datasets.

We designed five models of modular evolution for the egerniinae skink body plan to test integration and modularity via *EMMLi*. (1) a four-module model (*Body_Tail_Limbs_Head*) in which each of the major body regions is isolated as an independent module; (2) a three-module model (*BodyHead_Tail_Limbs*) where traits of the head and body are combined into a single module; (3) a two-module model (*BodyHeadTail_Limbs*) in which traits of
550 the head, body, and tail are combined into a single module; (4) a three-module model (*Body_Head_TailLimbs*) where tail and limb traits make up a single module; and (5) a two-module model (*BodyHead_TailLimbs*) where body and head traits are one module and tail and limb traits another.

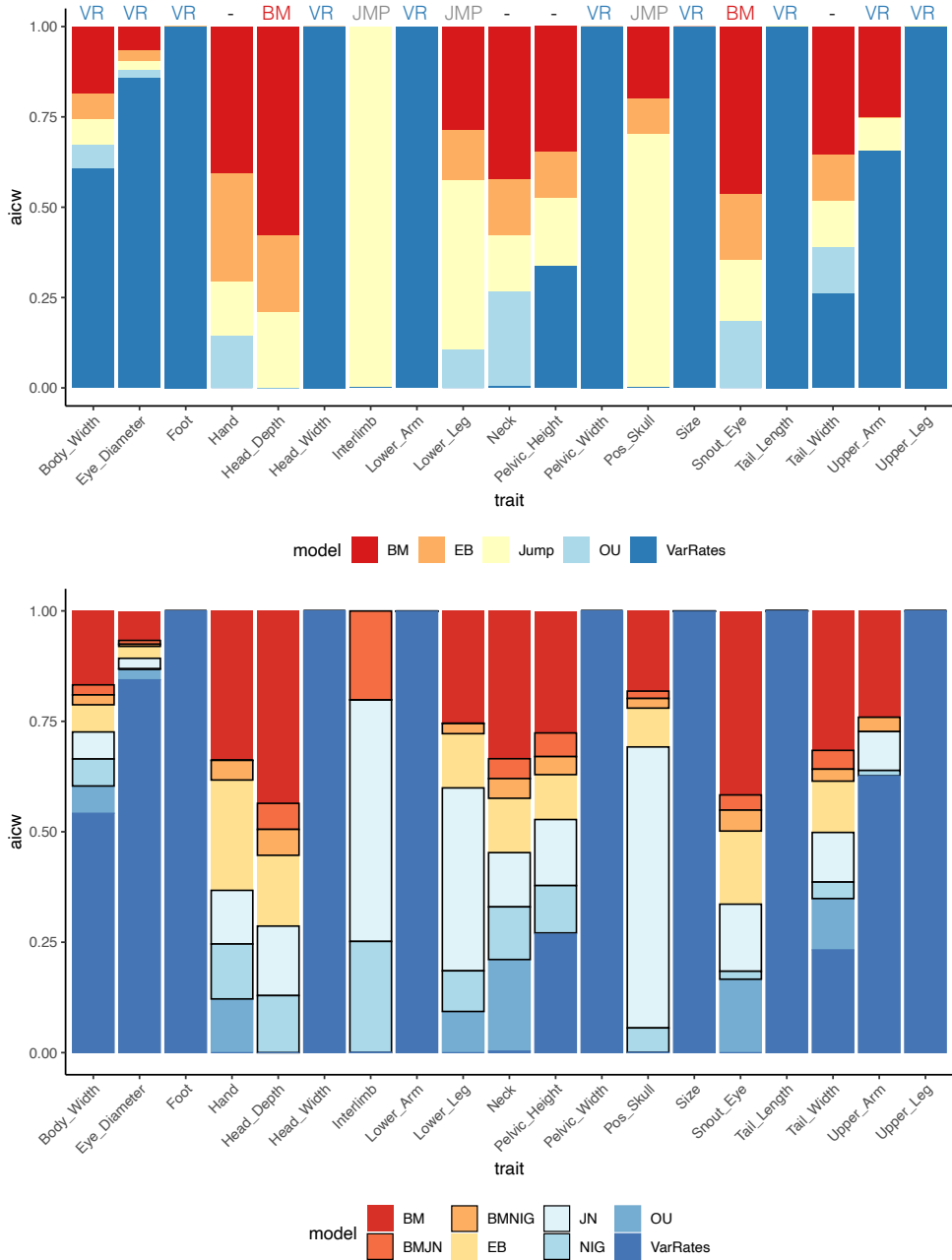


Figure S6: Comparative model fits for each of 19 morphological traits. Upper figure summarizes AICw by model type (BM, EB, ‘Jump’, OU, or VarRates), with the preferred model indicated above the column. Model preference required AICw of the best fitting model to be at least twice that of the next best fitting model. Bottom figure similarly shows model preference but with ‘Jump’ models expanded into their four alternative models (BMJN, BMNIG, JN, NIG) indicated by black outlines.

Concatenation and the Anomaly Zone



Figure S7: The Egerniinae phylogeny estimated from a concatenated and locus-partitioned alignment is likely misled by branches which fall into the anomaly zone. Colored branches correspond to the anomaly zone cladogram below and indicate edges which differ from the coalescent species tree.

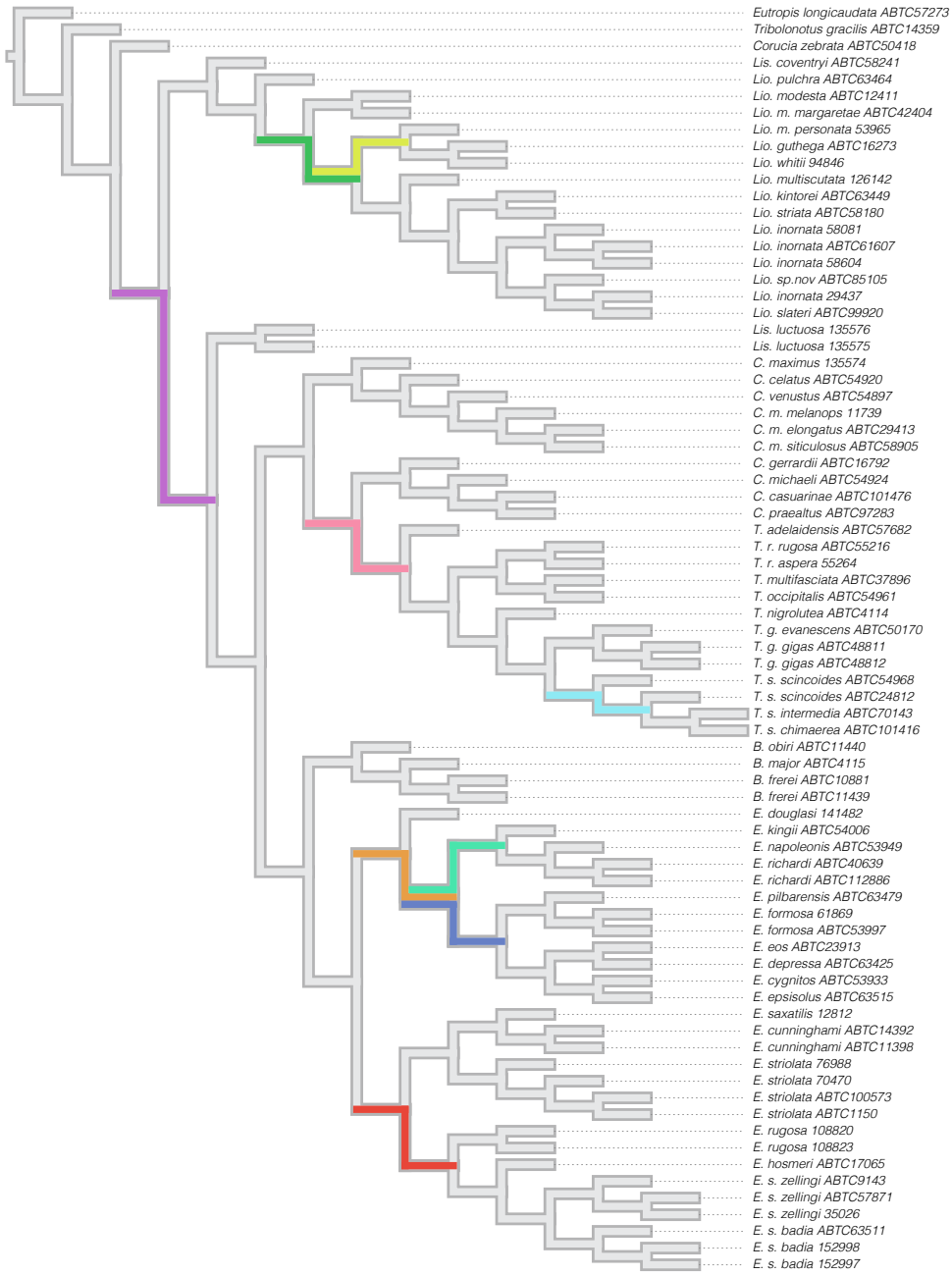


Figure S8: Colored branches indicate edges that fall within the anomaly zone and may provide misleading results under concatenation. We used *Anomaly Finder* [CITE Linkem et al. 2016], using the script from Chafin et al. 2021

560 **Topology Tests**

We used a series of topology tests in IQTREE to investigate two nodes which bear taxonomic implications. We used the concatenated alignment and simplified phylogenies as the input. In each case the preferred topology is presented first followed by the two alternative resolutions to the bipartition. Significant differences are denoted by (-), and show decisive preference 565 for the coalescent species tree topology in comparison to alternative resolutions, reinforcing molecular phylogenetic evidence for the paraphyly of both *Cyclodomorphus* and *Lissolepis*.

Topology test for the paraphyly of *Cyclodomorphus* with regards to *Tiliqua*.

Tree topologies:

- 570
1. (Egernia,(C.maximus,(T.gigas,C.michaeli)); : coalescent(concatenated species trees
 2. (Egernia,(C.michaeli,(T.gigas,C.maximus)); : alternative *Cyclodomorphus* paraphyly
 3. (Egernia,(T.gigas,(C.maximus,C.michaeli)); : *Cyclodomorphus* monophyly

Tree	logL	deltaL	bp-RELL	p-KH	p-SH	p-WKH	p-WSH	c-ELW	p-AU
1.	-1142007.338	0	0.97(+)	0.98(+)	1(+)	0.98(+)	0.993(+)	0.971(+)	0.981(+)
2.	-1142067.499	60.161	0.03(-)	0.02(-)	0.026(-)	0.02(-)	0.039(-)	0.0294(-)	0.021(-)
3.	-1142110.488	103.15	0(-)	0(-)	0(-)	0(-)	0(-)	2.08e-10(-)	1.79e-05(-)

Topology tests for the paraphyly of *Lissolepis*.

575 Tree topologies:

1. (Outgroup,((Lis.luctuosa,E.striolata),(Lis.coventryi,Lio._inornata))); : coalescent species tree
2. (Outgroup,(Lis.luctuosa,(E.striolata,(Lis.coventryi,Lio.inornata)))); : concatenated species tree
3. (Outgroup,((Lis.coventryi,Lis.luctuosa),(Lio.inornata,E.striolata))); : *Lissolepis* monophyly

Tree	logL	deltaL	bp-RELL	p-KH	p-SH	p-WKH	p-WSH	c-ELW	p-AU
1.	-1326723.218	0	1(+)	1(+)	1(+)	1(+)	1(+)	1(+)	0.995(+)
2.	-1326798.358	75.141	0(-)	0(-)	0.122(+)	0(-)	0(-)	8.47e-07(-)	0.00491(-)
3.	-1327315.329	592.11	0(-)	0(-)	0(-)	0(-)	0(-)	1.9e-174(-)	3.58e-05(-)

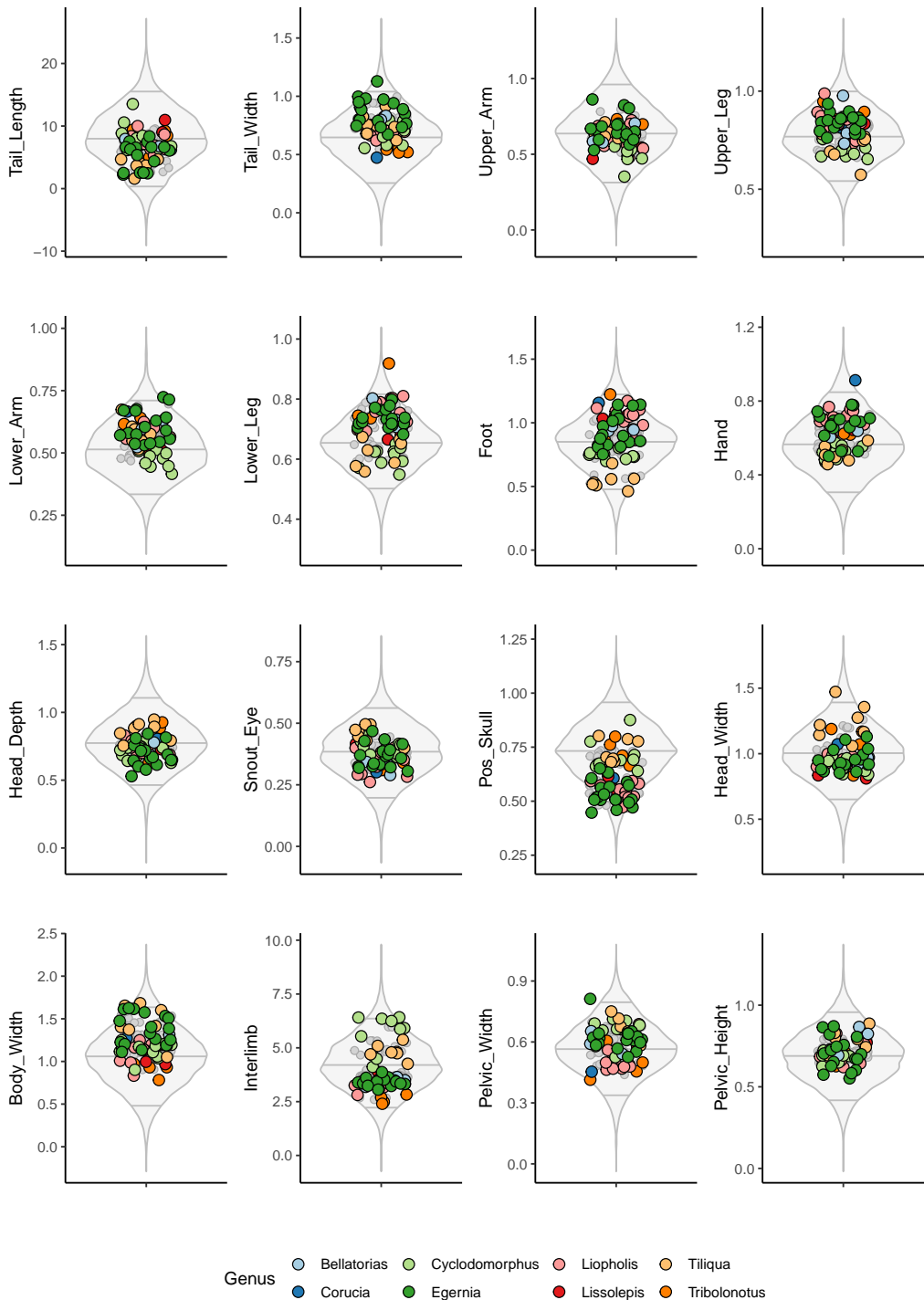


Figure S9: Empirical phenotypes generally conform to expected trait values of data simulated under uncorrelated evolution, showing limited ability of selection to exceed null expectations in Egerniinae skinks. Circles represent empirical trait values per species, colored by genus, with grey representing ancestral states. Transformed traits size corrected by log-shape ratios are plotted against 500 simulated datasets for each trait. Simulated traits are plotted as a grey violin plot summarizing the distribution of trait values, with 5%, 50%, and 95% quantiles plotted as horizontal lines. Simulations were generated with MVMORPH using as input the theta-root and sigma values estimated by MVMORPH assuming a constant-rate Brownian Motion model.

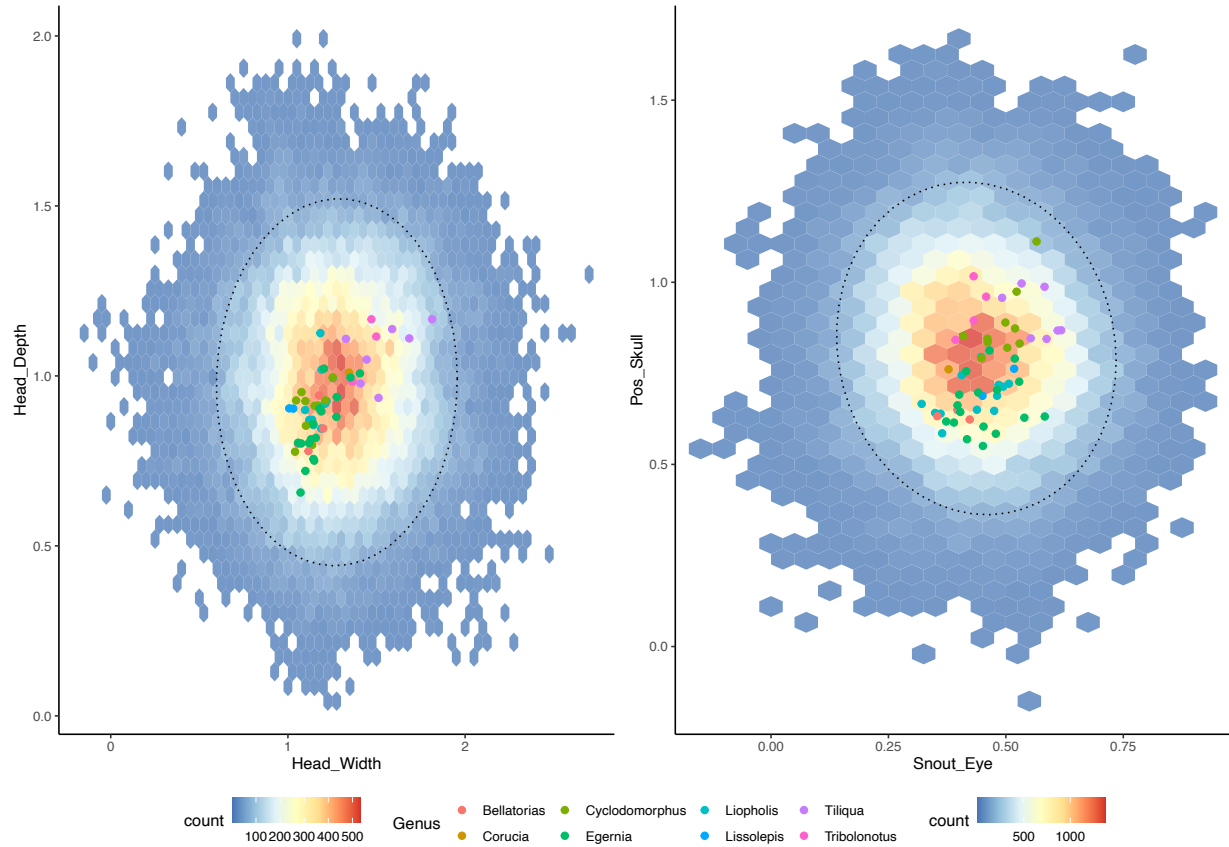


Figure S10: Empirical phenotypes generally conform to expected trait values of data simulated under uncorrelated evolution, showing limited ability of selection to exceed null expectations in Egerniinae skinks. Hexagonal heatmap in background shows the distribution of trait values from 500 datasets simulated under rates from empirical estimates. Warmer colors indicate greater density of simulated points. Circular points indicate empirical trait values and are colored according to the genus they belong to. The dotted ellipse contains 95% of the simulated data (95% confidence interval).

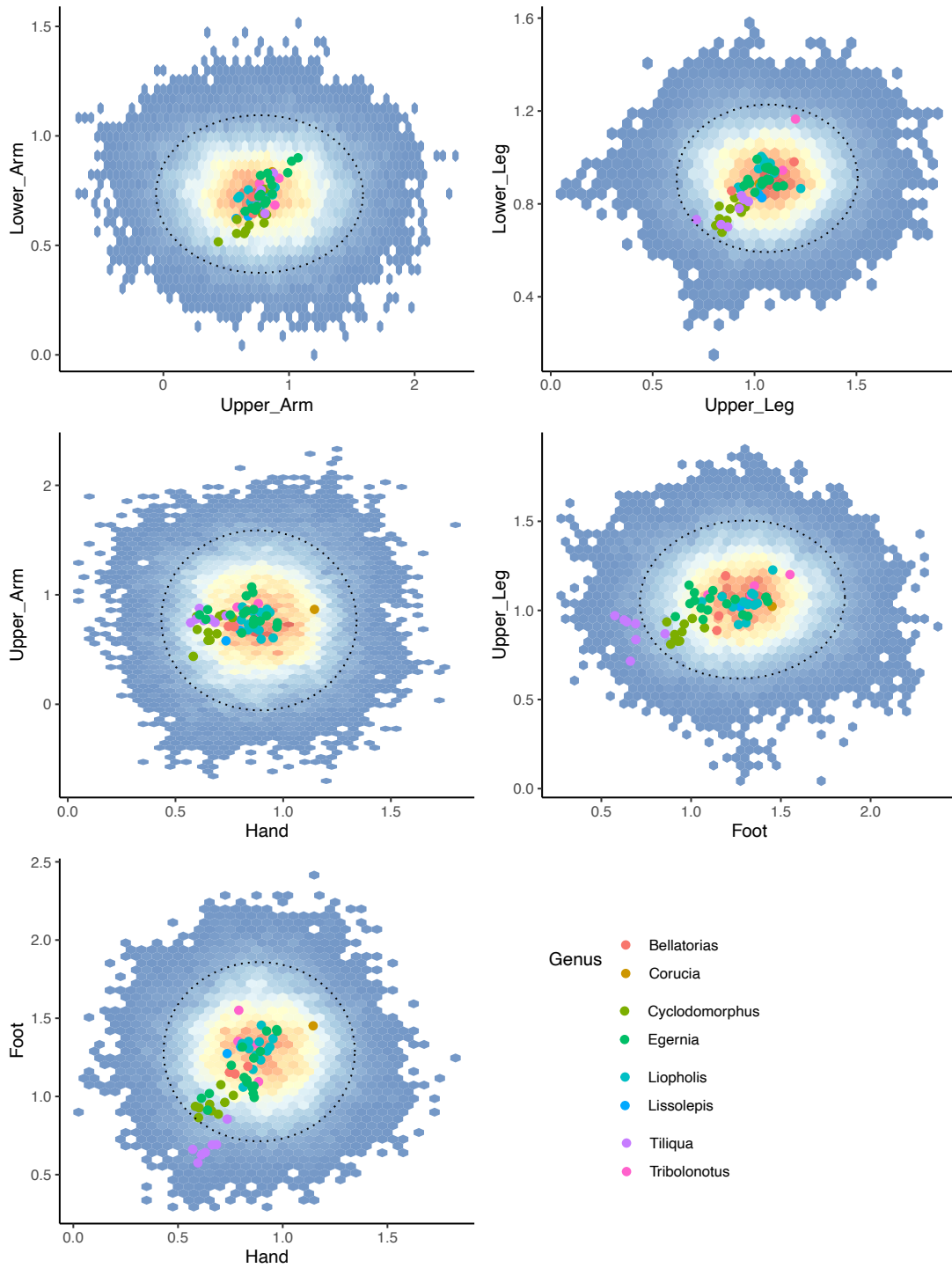


Figure S11: Empirical phenotypes generally conform to expected trait values of data simulated under uncorrelated evolution, showing limited ability of selection to exceed null expectations in Egerniinae skinks. Hexagonal heatplot in background shows the distribution of trait values from 500 datasets simulated under rates from empirical estimates. Warmer colors indicate greater density of simulated points. Circular points indicate empirical trait values and are colored according to the genus they belong to. The dotted ellipse contains 95% of the simulated data (95% confidence interval).

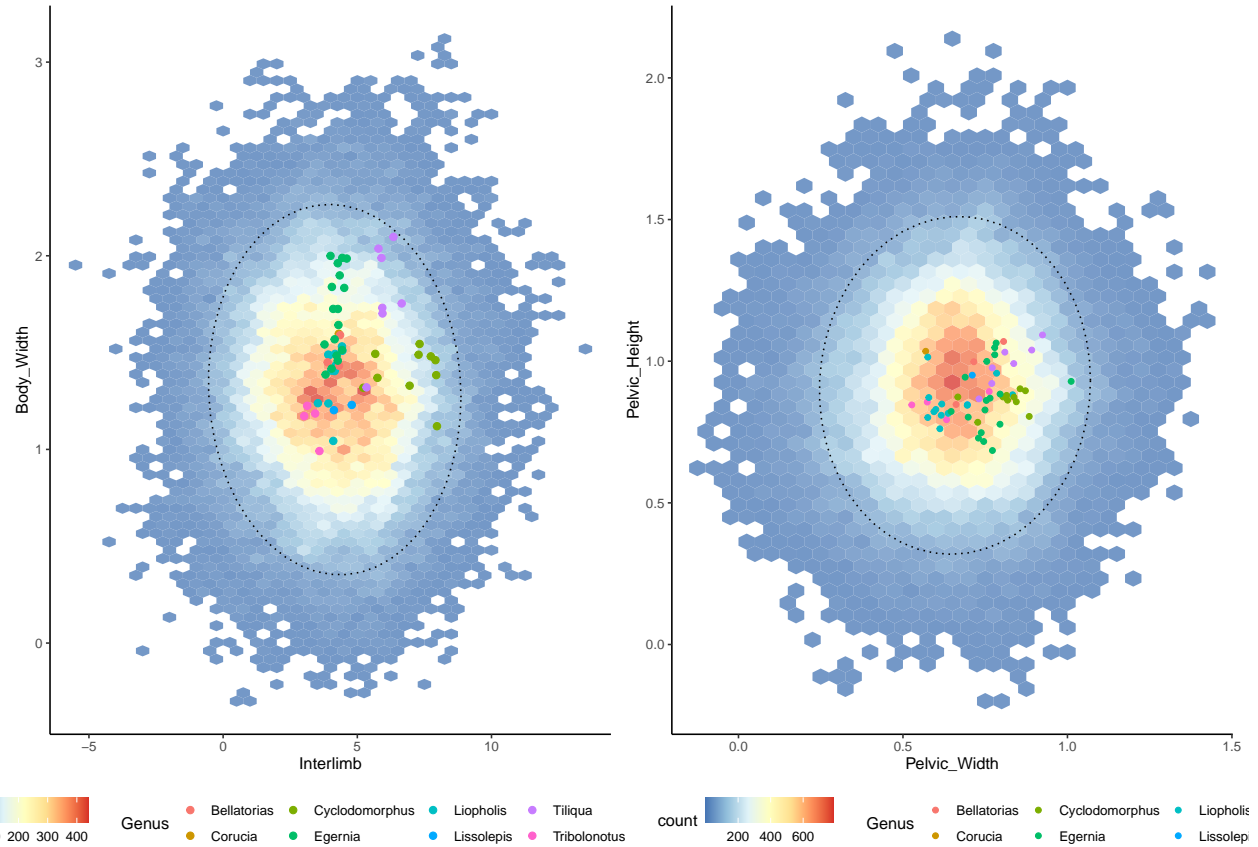


Figure S12: Empirical phenotypes generally conform to expected trait values of data simulated under uncorrelated evolution, showing limited ability of selection to exceed null expectations in Egerniinae skinks. Hexagonal heatplot in background shows the distribution of trait values from 500 datasets simulated under rates from empirical estimates. Warmer colors indicate greater density of simulated points. Circular points indicate empirical trait values and are colored according to the genus they belong to. The dotted ellipse contains 95% of the simulated data (95% confidence interval).

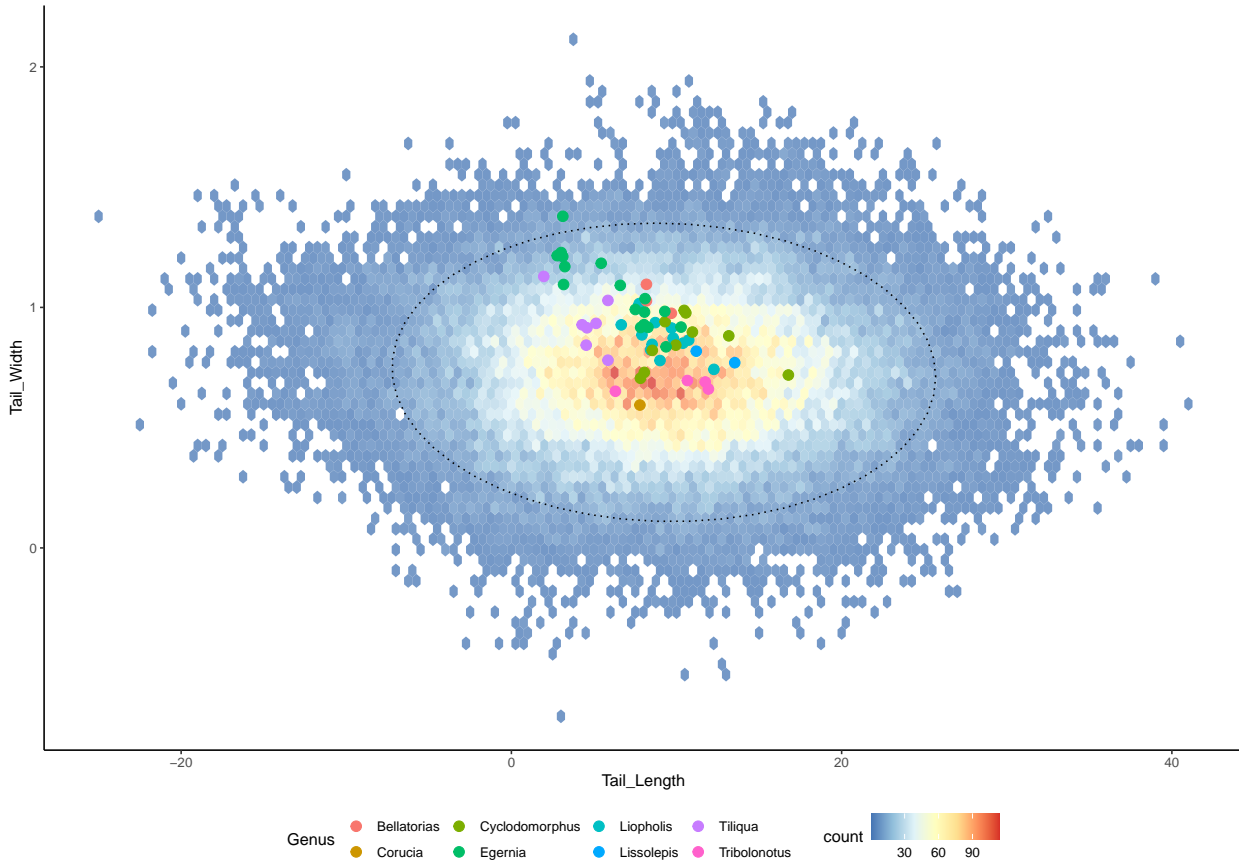


Figure S13: Empirical phenotypes generally conform to expected trait values of data simulated under uncorrelated evolution, showing limited ability of selection to exceed null expectations in Egerniinae skinks. Hexagonal heatmap in background shows the distribution of trait values from 500 datasets simulated under rates from empirical estimates. Warmer colors indicate greater density of simulated points. Circular points indicate empirical trait values and are colored according to the genus they belong to. The dotted ellipse contains 95% of the simulated data (95% confidence interval).

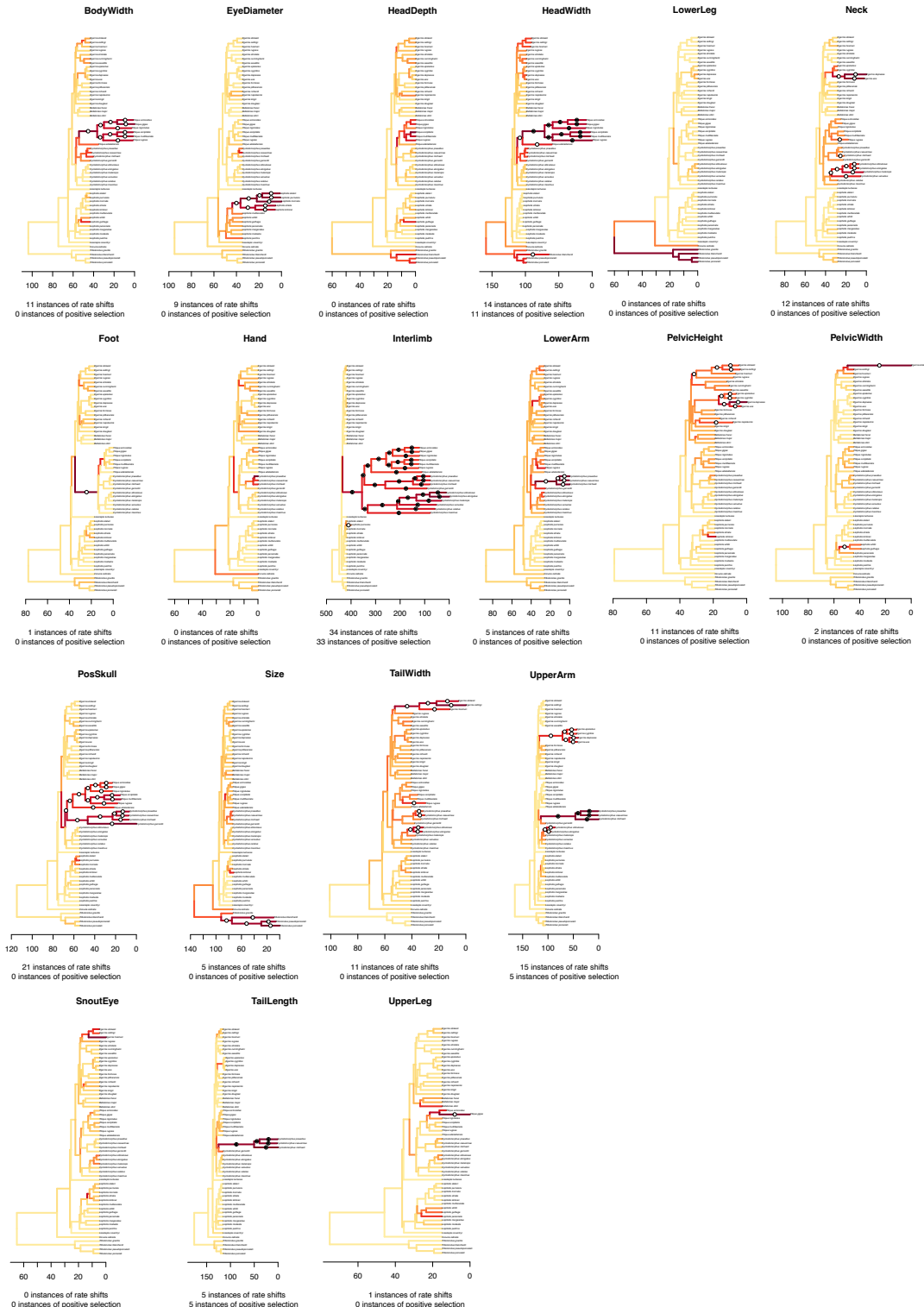


Figure S14: Pulses in rates of phenotypic evolution are common across egerniine morphological traits. Species trees have been transformed for each trait with branch lengths adjusted relative to the estimated Variable Rates median scalar. Branches are colored according to mean estimated sigma value. Circles indicate significant rate shifts: empty circles represent shifts which appeared in $> 70\%$ of the posterior samples and in which the mean estimated scalar > 2 ; black circles represent shifts which appeared in $> 95\%$ of the posterior samples and in which the mean estimated scalar > 2 corresponding to instances of “positive phenotypic selection” per Baker et al. 2017.

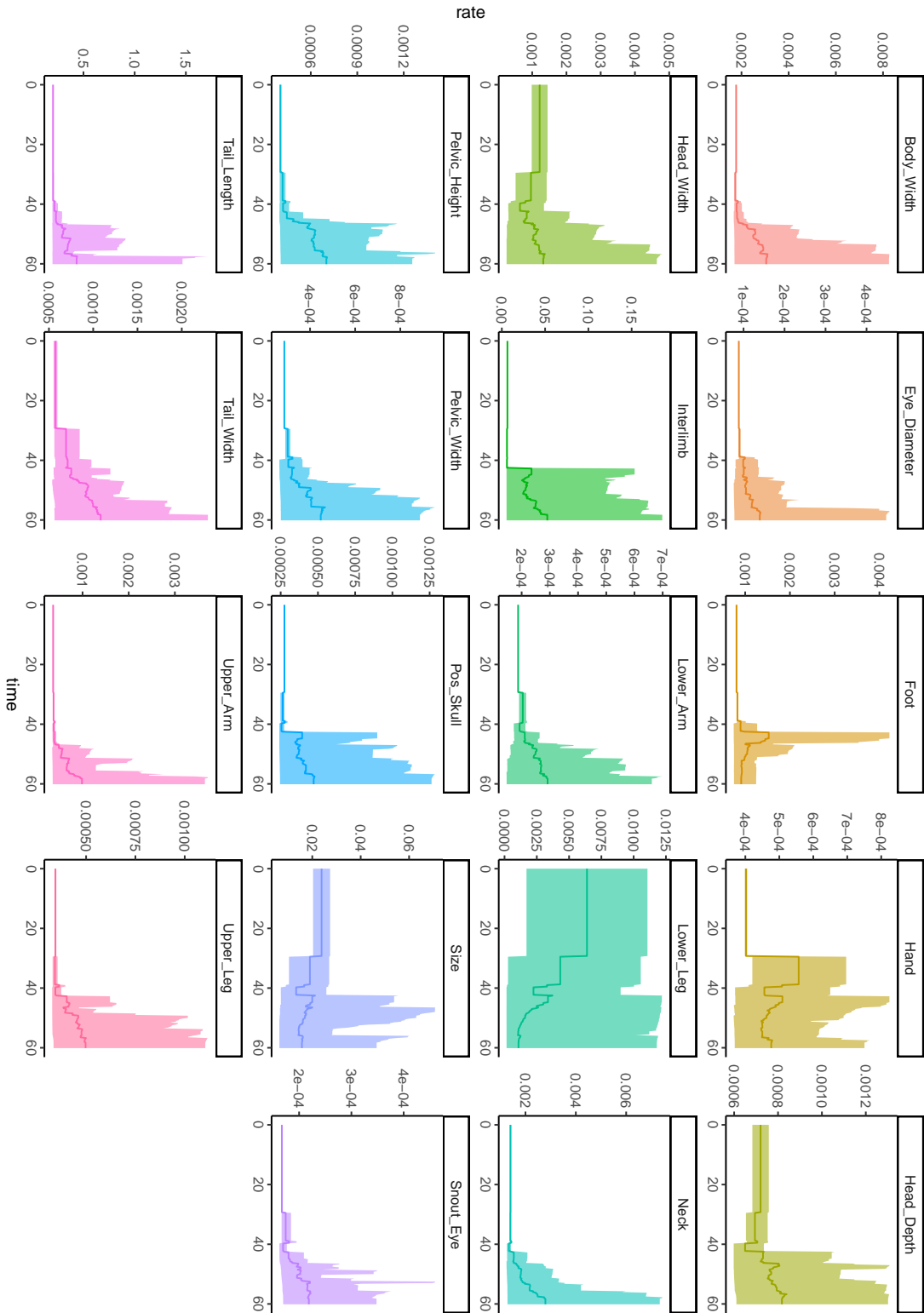


Figure S15: Mean evolutionary rates through time for all morphological traits with envelopes containing 95% quantiles.

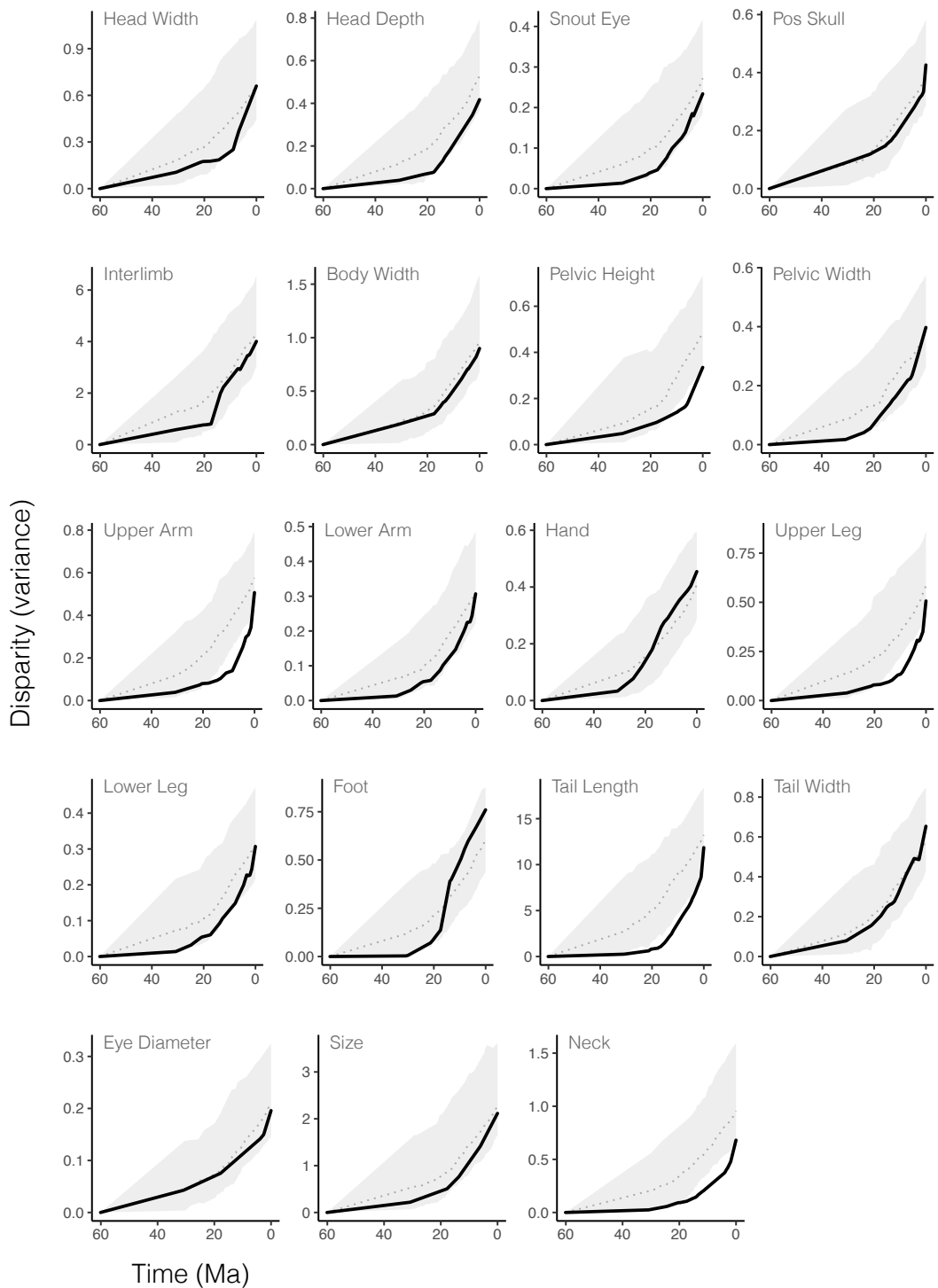


Figure S16: Disparity (variance) through time for morphological traits is often lower than expected under BM for long periods of time early in the evolution of this group. Empirical trends are shown in black with 95% quantiles of disparity for simulated datasets in grey.

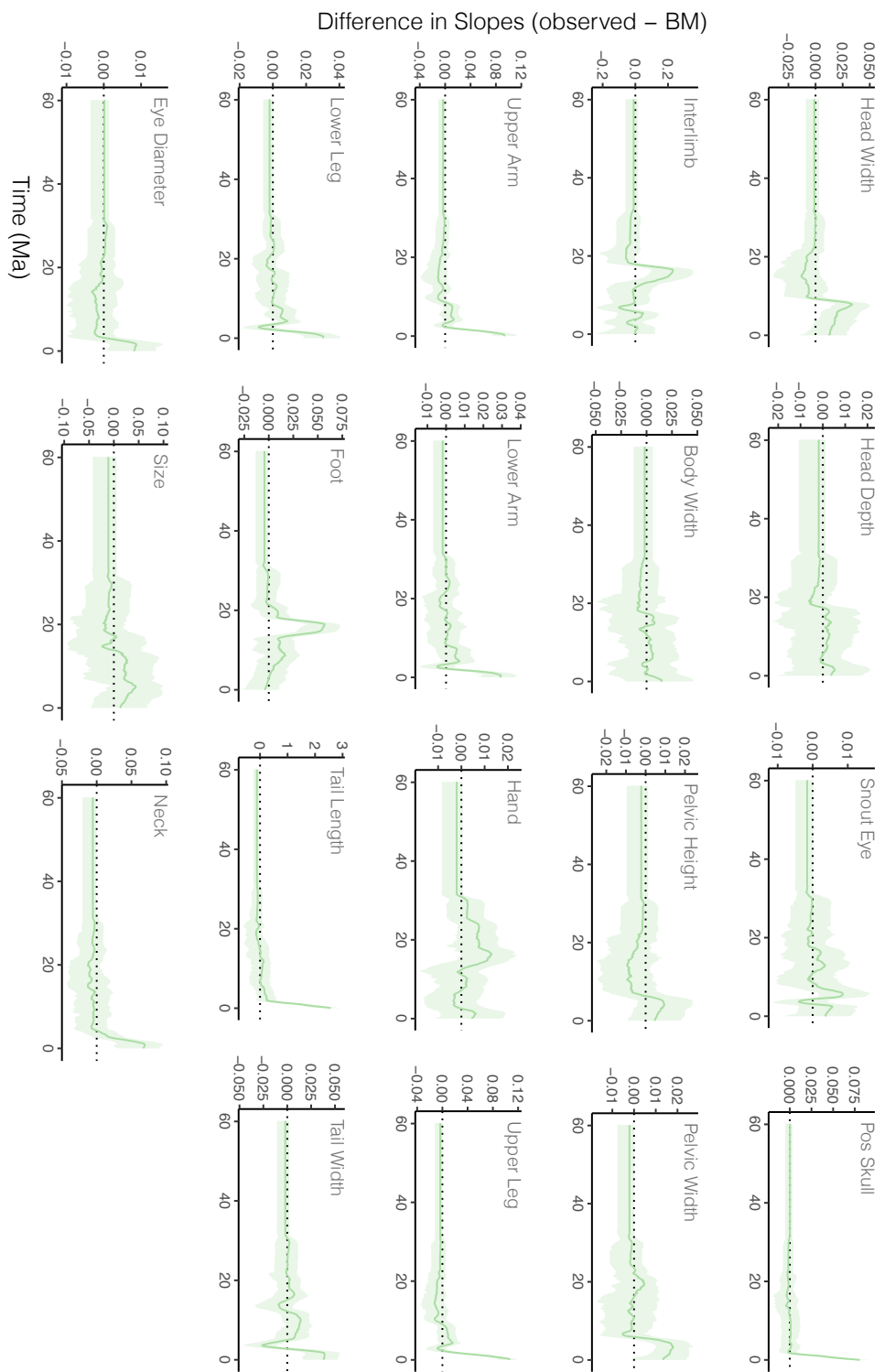


Figure S17: Individual traits show varied temporal patterns of morphological expansion and niche packing. Solid green line shows the mean trend and green envelope shows the 95% quantiles.

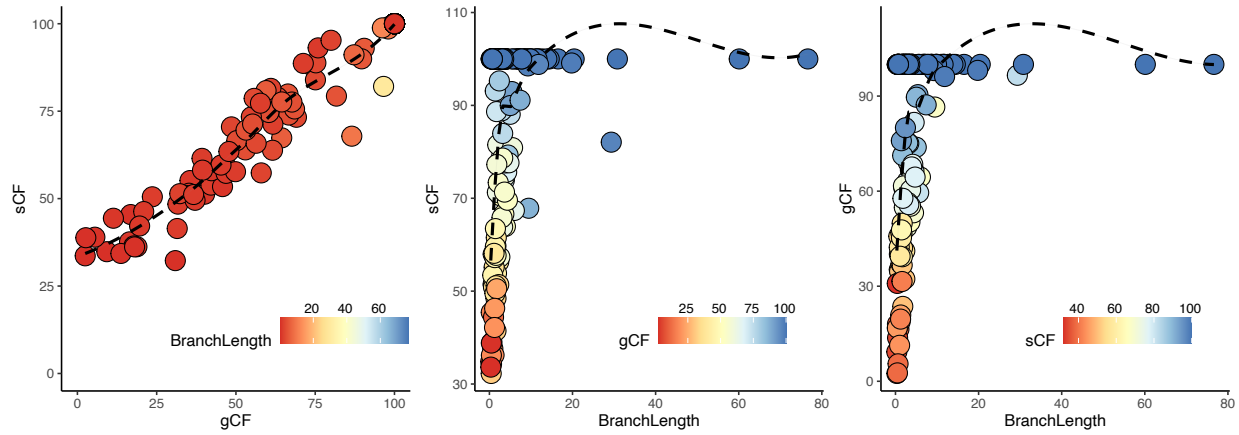


Figure S18: Concordance factors show a positive relationship with increasing branch length. Both site- and gene concordance factors increase support with increasing branch lengths (time), but show saturation ($sCF=100$, $gCF=100$) on branches ≥ 10 million years long.

References

- 580 Haeseler, A. von, Minh, B.Q. & Nguyen, M.A.T. (2013). Ultrafast approximation for phylogenetic bootstrap. *Molecular Biology and Evolution*, 30, 1188–1195.
- Lemmon, A.R., Emme, S.A. & Lemmon, E.M. (2012). Anchored hybrid enrichment for massively high-throughput phylogenomics. *Syst Biol*, 61, 727–44.
- 585 Schmidt, H.A., Minh, B.Q., Haeseler, A. von & Nguyen, L.-T. (2014). IQ-TREE: A fast and effective stochastic algorithm for estimating maximum-likelihood phylogenies. *Molecular Biology and Evolution*, 32, 268–274.
- Zhang, C., Sayyari, E. & Mirarab, S. (2017). ASTRAL-III: Increased scalability and impacts of contracting low support branches. In:, Comparative genomics. Conference Proceedings. Springer International Publishing, pp. 53–75.